Table 2
Experimental infection of H5N1 HPAI viruses in 4-week-old SPF pigs and virus recovery from nasal swabs.

Inoculated viruses	Virus titers on the dpi (log EID_{50}/ml)							
	0	1	2	3	4	5	6	7
Ws/Mongolia/3/05 (H5N1)	–[a]	3.3	3.8	2.0	2.6	3.8	2.6	–
	–	3.3	4.3	2.8	–	–	–	–
Ws/Mongolia/2/06 (H5N1)	–	0.8	2.8	3.0	3.3	4.5	5.0	3.8
	–	–	1.8	2.0	4.3	4.3	4.5	3.3
Ws/Mongolia/6/09 (H5N1)	–	3.5	2.8	–	≦1.3	1.5	–	–
	–	4.3	2.8	–	–	–	–	–

[a] –: <0.5 log EID50/ml.

intranasally inoculated at $10^{8.0}$ EID_{50} into six 4-week-old ducks (Table 3). Viruses were recovered from each of the tested samples of the ducks euthanized on 3 days post-inoculation (dpi). The titers of tissue samples from ducks infected with Ws/Mongolia/6/09 were relatively higher than those with Ws/Mongolia/3/05 or Ws/Mongolia/3/06. Three ducks of each group were kept for 14 days to observe the clinical signs of infected ducks. One of the 3 ducks infected with Ws/Mongolia/3/05 died on 9 dpi. Viruses were recovered only from the brain homogenate of this duck. Several neurological signs, such as depression, blindness, and intermittent head-shaking, were observed from 5 dpi onward in all ducks infected with Ws/Mongolia/3/05, and two recovered and survived on 14 dpi. For ducks infected with Ws/Mongolia/2/06, all three ducks survived during the experiment without showing any typical clinical signs. In contrast to the isolates in 2005 and 2006, the ducks infected with Ws/Mongolia/6/09 died earlier, on 4, 5, and 8 dpi, and showed depression and intermittent head-shaking before their death. Viruses were recovered from each of the tested tissues of dead ducks. Notably, the titers of tissue samples from 2 ducks that died on 4 and 5 dpi were clearly higher ($10^{7.5}$-$10^{9.5}$ EID_{50}/g) than those of the others.

Identification of avian influenza virus isolates from fecal samples of wild waterfowl

Since 2001 we have conducted surveillance studies on avian influenza in wild waterfowl in autumn at several lakes in Mongolia, including Khunt, Erkhel, Doityn Tsagaan, and Doroo Lakes, where migrating waterfowl congregate and H5N1 HPAI viruses were isolated from dead carcasses in 2005, 2006, and 2009. By 2009, 6,211 fecal samples of waterfowl had been collected and inoculated into chicken embryos. As a result, 338 avian influenza viruses of 10 different HA subtypes (H1, H2, H3, H4, H5, H7, H8, H9, H10, H12) were isolated, as shown in Table 4. A/duck/Mongolia/54/2001 (H5N2), A/duck/Mongolia/500/2001 (H5N3), and A/duck/Mongolia/596/2001 (H5N3) (underlined in Table 4) were isolated as H5 viruses in 2001. From sequence data of these isolates obtained previously (Soda et al., 2008), it was clear that the cleavage site of the HA of these H5 viruses had a low pathogenic profile without a pair of dibasic amino acid residues and these H5 viruses were genetically different from H5N1 HPAI virus isolates in Mongolia in phylogenetic analysis (Fig. 1). The results indicate that H5N1 HPAI viruses have not so far perpetuated at their nesting lakes in Siberia until 2009, since H5N1 HPAI viruses were isolated from migratory waterfowl only on their way back to their northern territory, not from those flying south from Siberia in autumn.

Discussion

Since 2005, numerous cases of H5N1 HPAI virus infection in wild birds have been found in Eurasian and African countries. The viruses of clades 2.2 and 2.2.1 are still epidemic in Asian and African countries in poultry and wild birds (WHO/OIE/FAO H5N1 Evolution Working Group, 2009). This suggests that H5N1 viruses prevailing in domestic birds have transmitted to wild migratory waterfowl by water-borne transmission repeatedly and it was a concern that these H5N1 viruses may perpetuate among migratory waterfowl and in their nesting lake water in nature. In Mongolia, H5N1 viruses of clade 2.2 were isolated from waterfowl spontaneously in 2005 and 2006 after the infections in Qinghai Lake, China. In May and July 2009, H5N1 viruses of clade 2.3.2 were isolated from whooper swans, bar-headed goose, common goldeneye, and ruddy shelduck at Doityn Tsagaan and Doroo Lakes. Furthermore, H5N1 viruses of clade 2.3.2 were isolated again from whooper swans at Ganga Lake in May 2010. H5N1 viruses of clade 2.3.2 were first identified from ducks, geese and other mammals in China and Vietnam in 2005 (Chen et al., 2006; Roberton et al., 2006). In addition, H5N1 viruses of clades 2.3.2 and 2.3.4 were isolated from wild birds in Hong Kong (Ellis et al., 2009; Smith et al., 2009). H5N1 viruses of clade 2.3.2 were also isolated in Japan, Korea, and Russia in 2008 from whooper swan (L'Vov et al., 2008; Uchida et al., 2008). In the present study, genetic analyses indicate that H5N1 isolates in Mongolia in 2009 and 2010 were closely related with those in Russia, China, Laos, and Japan. In particular, the homologies of nucleotides of each segment between Ws/Mongolia/6/09 and A/grebe/Tyva/3/2009 (H5N1), which was isolated in Russia (accession No. GQ386142–GQ386149), ranged from 99.8% to 99.9%. It is clear that these waterfowl were infected with the same H5N1 viruses in southern areas and flew north since the place and date of outbreaks were closely related according to information from the OIE (2009b). In addition, waterfowl were infected again with the similar H5N1 viruses of clade 2.3.2 in southern areas and flied to the north in 2010. H5N1 viruses isolated from wild birds in Hong Kong in 2007 and 2008 also showed high homology with H5N1 isolates in Mongolia in 2009 and 2010, suggesting that the origin of these viruses was H5N1 viruses prevailing in domestic poultry in China, and those progeny viruses must have transmitted to wild migratory waterfowl by water-borne transmission every year.

Table 3
Experimental infection of H5N1 HPAI viruses in 4-week-old domestic ducks and virus recovery from organs.

Inoculated viruses	No. of ducks	dpi (Health status)	Virus titers of organs (log EID_{50}/g)				
			Brain	Trachea	Lungs	Kidneys	Colon
Ws/Mongolia/3/05 (H5N1)	3	3 (sacrificed)	4.5, 5.3, 6.3	4.0, 5.5, 6.3	4.0, 5.5, 6.3	5.8, 6.3, 6.5	4.3, 4.6, 4.8
	1[a]	9 (dead)	3.3	–[b]	–	–	–
	2[a]	14 (sacrificed)	–,–	–,–	–,–	–,–	–,–
Ws/Mongolia/2/06 (H5N1)	3	3 (sacrificed)	2.3, 3.8, 3.8	4.0, 4.3, 4.3	4.0, 4.3, 4.3	3.5, 4.3, 5.0	3.5, 4.0, 4.0
	3[c]	14 (sacrificed)	–,–,–	–,–,–	–,–,–	–,–,–	–,–,–
Ws/Mongolia/6/09 (H5N1)	3	3 (sacrificed)	4.3, 7.3, 7.3	5.7, 6.8, 8.5	6.5, 6.8, 7.8	6.0, 7.5, 8.3	4.8, 5.8, 7.6
	1[a]	4 (dead)	9.5	9.3	8.5	8.5	8.5
	1[a]	5 (dead)	8.3	7.5	9.5	8.3	8.3
	1[a]	8 (dead)	3.8	5.5	4.5	3.0	3.5

[a] Each duck showed depression, blindness, and head-shaking.
[b] <1.5 log EID50/g.
[c] One of the three ducks showed depression and blindness at 5-8 dpi and survived for 14 days.

Table 4
Isolation of avian influenza viruses from fecal samples of migratory waterfowl in Mongolia.

Sampling date	Name of lakes	Isolated viruses/Total samples	Subtypes of viruses[a] (No. of isolates)
Sep., 2001	Ugii, Doityn tsagaan,	37/725	H1N1 (1), H3N2 (1), H3N6 (3), H3N8 (11), H4N2 (1), H4N6 (12), H5N2 (1), H5N3 (2), H7N1 (1), H10N3 (4)
Sep., 2002	Erkhel, Ugii	109/959	H1N1 (3), H3N3 (2), H3N6 (20), H3N8 (53), H4N6 (12), H4N7 (1), H4N8 (1), H7N1 (1), H7N7 (9), H8N4 (5), H10N7 (1), H12N5 (1)
Sep., 2003	Ugii,	68/750	H1N1 (1), H2N3 (1), H3N6 (6), H3N8 (28), H4N2 (1), H4N6 (25), H9N2 (1), H10N5 (5)
Sep., 2005	Ugii,	32/476	H3N2 (1), H3N6 (2), H3N8 (10), H4N6 (6), H8N4 (1), H10N3 (11), H10N7 (5)
Aug., 2006	Khunt, Ugii, Borgin, Shorvog, Baga Tsaisam, Duut, Ikh Tsaidam, Doityn tsagaan	18/545	H2N2 (1), H3N8 (8), H4N6 (9)
Aug., 2007	Khunt, Ugii, Dunt, Ikh Tsaidam, Doityn tsagaan	20/943	H3N8 (14), H4N3(1), H7N6 (1), H7N7 (4)
Aug., 2008	Khunt, Ugii, Dunt, Ikh Tsaidam, Doityn tsagaan	40/792	H3N6 (3), H3N8 (23), H4N6 (8), H4N8 (3), H7N9 (3)
Aug., 2009	Ugii, Doityn tsagaan, Khunt Doroo, Sharga	9/1021	H1N8 (1), H3N8 (2), H4N6 (3), H8N4 (3)

[a] H5 isolates, A/duck/Mongolia/54/2001 (H5N2), A/duck/Mongolia/500/2001 (H5N3), and A/duck/Mongolia/596/2001 (H5N3), were underlined.

All cases of H5N virus infection in 2005, 2006, 2009, and 2010 were in May and July, when wild waterfowl migrate from the southern Asia to their nesting lakes in Siberia. In addition, H5N1 viruses genetically related to the isolates in Mongolia were prevailing in domestic poultry in the southern Asia, although no outbreak of HPAI was so far reported in poultry in Mongolia. Furthermore, the results of intensive surveillance of avian influenza in migratory waterfowl flying from their nesting lakes in Siberia to Mongolia in every autumn indicate that no HPAI virus has been isolated from wild waterfowl flying from their nesting lakes until 2009. These results demonstrate that wild waterfowl were sporadically infected with H5N1 HPAI viruses prevailing in domestic poultry in the southern Asia and died in Mongolia on the way back to their northern territory in spring and no HPAI virus has perpetuated at their nesting lakes in Siberia until 2009. To reduce the risk of the perpetuation of HPAI viruses among migratory waterfowl at their nesting lakes in Siberia, HPAI viruses should be contained within poultry in the southern Asia by a stamping-out strategy, the basic control measure of HPAI.

It was proposed that the expression of sialic acid receptors for human and avian influenza viruses on epithelial cells of the trachea renders pigs susceptible to infection with both types of influenza viruses (Ito et al., 1998). From the previous experience of pandemic influenza, pigs play an important role as a "mixing vessels" to generate pandemic influenza virus as a genetic reassortant between avian and human influenza viruses (Kida et al., 1988, 1994). In this experiment, all 3 H5N1 viruses replicated in pigs, but the titers of nasal swabs and the period of virus shedding were lower than the infections with swine influenza viruses (Bai et al., 2005). Although the susceptibility of domestic pigs to H5N1 avian influenza viruses is not high (Isoda et al., 2006; Lipatov et al., 2008), natural pig-to-pig infections with H5N1 avian influenza viruses have been found (Choi et al., 2005; Takano et al., 2009). A surveillance study of influenza virus infection in pigs should be promoted to assess the prevalence of H5N1 viruses in pigs and the pathogenicity of these isolates in mammals and birds for future pandemics in humans.

Originally, non-pathogenic avian influenza viruses isolated from migratory waterfowl replicated only in columnar epithelial cells, forming crypts in the large intestine, and were excreted in the fecal materials (Kida et al., 1980; Webster et al., 1978). In the case of H5N1 HPAI viruses, recent isolates acquired lethal pathogenicity in waterfowl, although previous H5N1 isolates also replicated systemically and did not show lethal clinical signs in ducks (Chen et al., 2004; Hulse-Post et al., 2005; Kim et al., 2008; Pantin-Jackwood et al., 2007; Sturm-Ramirez et al., 2005). In the present study, we examined the pathogenicity of Ws/Mongolia/3/05 (clade 2.2), Ws/Mongolia/2/06 (clade 2.2), and Ws/Mongolia/6/09 (clade 2.3.2) of H5N1 viruses in domestic ducks. To assess the pathogenicity of avian influenza in ducks, the age and strain of ducks, infectivity titers of the inocula, and the route of inoculation influence the results (Keawcharoen et al., 2008; Kim et al., 2008; Pantin-Jackwood et al., 2007). In our studies, including previous experiments (Kishida et al., 2005), H5 avian influenza viruses of $10^{8.0}$ EID_{50} were inoculated intranasally into 4-week-old domestic ducks of Chelly Valley strain. It is noted that systemic replication with low mortality of Ws/Mongolia/3/05 and Ws/Mongolia/2/06, and high mortality of Ws/Mongolia/6/09 was observed as compared with previous reports (Brown et al., 2006; Kishida et al., 2005; Pfeiffer et al., 2009). The present results support that H5N1 influenza viruses have evolved to cause lethal infection in ducks since multiple infections of domestic ducks and wild birds with these viruses have continued in epidemic areas. Further investigation on the H5N1 virus infections in wild birds is needed in addition to the recent studies (Hulse-Post et al., 2007; Reed et al., 2010) since they are not sufficient to understand on the molecular basis of the pathogenicity of these H5N1 isolates in ducks.

In conclusion, H5N1 HPAI viruses were isolated from migratory waterfowl only on their way back to their northern territory, and not from those flying to the south from Siberia in autumn, suggesting that H5N1 HPAI viruses have not perpetuated at their nesting lakes in Siberia until 2009. For the control of influenza virus infection in birds and mammals, the global surveillance to understand the ecology of influenza viruses and stamping out policy to contain the HPAI viruses in the domestic poultry are essential.

Materials and methods

Isolation and identification of viruses

Virus isolation was carried out from the homogenate of the brain, lungs, spleen of bar-headed goose (*Anser indicus*), whooper swan (*Cygnus cygnus*), common goldeneye (*Bucephala clangula*), and ruddy shelduck (*Tadorna ferruginea*), which were found as carcasses in the Khunt, Erkhel, Doityn Tsagaan, Doroo, and Ganga Lakes, Mongolia in July 2005, May 2006, May 2009, July 2009, and May 2010 (Table 1). Ten percent organ homogenates were inoculated into the allantoic cavities of 10-day-old chicken embryos. Subtypes of influenza virus isolates were identified by hemagglutination-inhibition (HI) and neuraminidase-inhibition (NI) tests using antisera to the reference strains of influenza viruses (Kida and Yanagawa, 1979).

A total of 6,211 fecal samples was collected from waterfowl in 2001–2009 in Mongolia. Each sample was mixed with minimum essential medium (MEM) containing antibiotics and inoculated into the allantoic cavities of 10-day-old chicken embryos. Subtypes of influenza virus isolates were identified by HI and NI tests as described above.

Sequencing and phylogenetic analysis

Viral RNA was extracted from the allantoic fluid of chicken embryos infected with viruses by TRIzol LS Reagent (Invitrogen) and reverse-transcribed with the Uni12 primer (Hoffmann et al., 2001) and M-MLV Reverse Transcriptase (Invitrogen). The full-length genome of each gene segment was amplified by polymerase chain reaction with gene-specific primer sets (Hoffmann et al., 2001). Direct sequencing of each gene segment was performed using an auto sequencer, CEQ 2000XL (Beckman Coulter). The nucleotide sequences of H5 isolates obtained in the present study have been registered in GenBank/EMBL/DDBJ, as shown in Table 1.

To assess genetic relationship among H5 influenza virus strains, the sequence of 976 bp of the HA gene of each isolate was compared with those of H5 viruses from our previous study (Soda et al., 2008) and the public database. Phylogenetic tree was constructed by the neighbor-joining method (Saitou and Nei, 1987).

Experimental infection of chickens, pigs, and domestic ducks with H5N1 isolates

To assess the pathogenicity of H5N1 isolates, each virus was inoculated into chickens (*Gallus gallus*), pigs (*Sus scrofa domestic*), and domestic ducks (*Anas platyrhynchos var. domesuticus*), respectively. For the intravenous pathogenicity index (IVPI) test, 0.1 ml of 1:10 dilutions of infectious allantoic fluids were inoculated intravenously into ten 6- or 7-week-old chickens (Boris brown, Japan). The IVPI was calculated according to the standard protocol (OIE, 2009a).

For the pathogenicity test in pigs, 1 ml of each H5N1 isolate containing $10^{8.0}$ EID_{50} was inoculated intranasally into two 4-week-old specific pathogen-free pigs (Sankyo Lab Service, Japan) and nasal swabs of each pig were collected daily in 2 ml MEM containing antibiotics from 1 to 7 dpi for virus recovery.

For the pathogenicity test in ducks, 0.1 ml of each H5N1 isolate containing $10^{8.0}$ EID_{50} was inoculated intranasally into six 4-week-old ducks (Chelly Valley, Japan). Three of the ducks were euthanized on 3 dpi and the brain, trachea, lungs, kidneys and colon were collected aseptically for virus recovery. The remaining 3 ducks were observed clinically for 14 days after inoculation. On the death of ducks, their tissues were collected for virus recovery. The sera and organs were collected from survived ducks for antibody response and virus recovery. Swab samples of pigs and tissue homogenates from ducks were inoculated into 10-day-old embryonated chicken eggs and virus titers were calculated and expressed as the EID_{50} per ml (swab) or gram (tissue). For the evaluation of immune response, specific antibodies were detected by hemagglutination-inhibition test in 0.025 ml of collected duck sera according to the standard protocol (OIE, 2009a).

Each animal was housed in a self-contained isolator unit (Tokiwa Kagaku, Japan) at a BSL-3 facility at the Graduate School of Veterinary Medicine, Hokkaido University, Japan.

Acknowledgments

The authors are grateful to Takikawa Shinseien (Hokkaido, Japan) for providing domestic ducks for experimental infection studies. The authors are also grateful to Ms. C. Yamamoto for her support of the surveillance study in Mongolia. We also thank Ms. M. Jizou, Ms. H. Shibuya, Ms. H. Yoshida, Ms. M. Endo, Ms. Y. Sato, and Ms. H. Miyamoto, Hokkaido University, for their technical support. The present work was supported in part by the Program of Founding Research Centers for Emerging and Reemerging Infectious Disease from the Ministry of Education, Culture, Sports, Science, and Technology, Japan, and the Japan Racing and Livestock Promotion Foundation.

References

Bai, G.R., Sakoda, Y., Mweene, A.S., Kishida, N., Yamada, T., Minakawa, H., Kida, H., 2005. Evaluation of the ESPLINE INFLUENZA A&B-N Kit for the diagnosis of avian and swine influenza. Microbiol. Immunol. 49, 1063–1067.

Brown, J.D., Stallknecht, D.E., Beck, J.R., Suarez, D.L., Swayne, D.E., 2006. Susceptibility of North American ducks and gulls to H5N1 highly pathogenic avian influenza viruses. Emerg. Infect. Dis. 12, 1663–1670.

Chen, H., Deng, G., Li, Z., Tian, G., Li, Y., Jiao, P., Zhang, L., Liu, Z., Webster, R.G., Yu, K., 2004. The evolution of H5N1 influenza viruses in ducks in southern China. Proc. Natl Acad. Sci. USA 101, 10452–10457.

Chen, H., Smith, G.J., Li, K.S., Wang, J., Fan, X.H., Rayner, J.M., Vijaykrishna, D., Zhang, J.X., Zhang, L.J., Guo, C.T., Cheung, C.L., Xu, K.M., Duan, L., Huang, K., Qin, K., Leung, Y.H., Wu, W.L., Lu, H.R., Chen, Y., Xia, N.S., Naipospos, T.S., Yuen, K.Y., Hassan, S.S., Bahri, S., Nguyen, T.D., Webster, R.G., Peiris, J.S., Guan, Y., 2006. Establishment of multiple sublineages of H5N1 influenza virus in Asia: implications for pandemic control. Proc. Natl Acad. Sci. USA 103, 2845–2850.

Chen, H., Smith, G.J., Zhang, S.Y., Qin, K., Wang, J., Li, K.S., Webster, R.G., Peiris, J.S., Guan, Y., 2005. Avian flu: H5N1 virus outbreak in migratory waterfowl. Nature 436, 191–192.

Choi, Y.K., Nguyen, T.D., Ozaki, H., Webby, R.J., Puthavathana, P., Buranathal, C., Chaisingh, A., Auewarakul, P., Hanh, N.T., Ma, S.K., Hui, P.Y., Guan, Y., Peiris, J.S., Webster, R.G., 2005. Studies of H5N1 influenza virus infection of pigs by using viruses isolated in Vietnam and Thailand in 2004. J. Virol. 79, 10821–10825.

Ellis, T.M., Bousfield, R.B., Bissett, L.A., Dyrting, K.C., Luk, G.S., Tsim, S.T., Sturm-Ramirez, K., Webster, R.G., Guan, Y., Malik Peiris, J.S., 2004. Investigation of outbreaks of highly pathogenic H5N1 avian influenza in waterfowl and wild birds in Hong Kong in late 2002. Avian Pathol. 33, 492–505.

Ellis, T.M., Dyrting, K.C., Wong, C.W., Chadwick, B., Chan, C., Chiang, M., Li, C., Li, P., Smith, G.J., Guan, Y., Malik Peiris, J.S., 2009. Analysis of H5N1 avian influenza infections from wild bird surveillance in Hong Kong from January 2006 to October 2007. Avian Pathol. 38, 107–119.

Hoffmann, E., Stech, J., Guan, Y., Webster, R.G., Perez, D.R., 2001. Universal primer set for the full-length amplification of all influenza A viruses. Arch. Virol. 146, 2275–2289.

Hulse-Post, D.J., Franks, J., Boyd, K., Salomon, R., Hoffmann, E., Yen, H.L., Webby, R.J., Walker, D., Nguyen, T.D., Webster, R.G., 2007. Molecular changes in the polymerase genes (PA and PB1) associated with high pathogenicity of H5N1 influenza virus in mallard ducks. J. Virol. 81, 8515–8524.

Hulse-Post, D.J., Sturm-Ramirez, K.M., Humberd, J., Seiler, P., Govorkova, E.A., Krauss, S., Scholtissek, C., Puthavathana, P., Buranathai, C., Nguyen, T.D., Long, H.T., Naipospos, T.S., Chen, H., Ellis, T.M., Guan, Y., Peiris, J.S., Webster, R.G., 2005. Role of domestic ducks in the propagation and biological evolution of highly pathogenic H5N1 influenza viruses in Asia. Proc. Natl Acad. Sci. USA 102, 10682–10687.

Isoda, N., Sakoda, Y., Kishida, N., Bai, G.R., Matsuda, K., Umemura, T., Kida, H., 2006. Pathogenicity of a highly pathogenic avian influenza virus, A/chicken/Yamaguchi/7/04 (H5N1) in different species of birds and mammals. Arch. Virol. 151, 1267–1279.

Ito, T., Couceiro, J.N., Kelm, S., Baum, L.G., Krauss, S., Castrucci, M.R., Donatelli, I., Kida, H., Paulson, J.C., Webster, R.G., Kawaoka, Y., 1998. Molecular basis for the generation in pigs of influenza A viruses with pandemic potential. J. Virol. 72, 7367–7373.

Ito, T., Okazaki, K., Kawaoka, Y., Takada, A., Webster, R.G., Kida, H., 1995. Perpetuation of influenza A viruses in Alaskan waterfowl reservoirs. Arch. Virol. 140, 1163–1172.

Keawcharoen, J., van Riel, D., van Amerongen, G., Bestebroer, T., Beyer, W.E., van Lavieren, R., Osterhaus, A.D., Fouchier, R.A., Kuiken, T., 2008. Wild ducks as long-distance vectors of highly pathogenic avian influenza virus (H5N1). Emerg. Infect. Dis. 14, 600–607.

Kida, H., Ito, T., Yasuda, J., Shimizu, Y., Itakura, C., Shortridge, K.F., Kawaoka, Y., Webster, R.G., 1994. Potential for transmission of avian influenza viruses to pigs. J. Gen. Virol. 75, 2183–2188.

Kida, H., Kawaoka, Y., Naeve, C.W., Webster, R.G., 1987. Antigenic and genetic conservation of H3 influenza virus in wild ducks. Virology 159, 109–119.

Kida, H., Shortridge, K.F., Webster, R.G., 1988. Origin of the hemagglutinin gene of H3N2 influenza viruses from pigs in China. Virology 162, 160–166.

Kida, H., Yanagawa, R., 1979. Isolation and characterization of influenza a viruses from wild free-flying ducks in Hokkaido. Jpn. Zentralbl. Bakteriol. A. 244, 135–143.

Kida, H., Yanagawa, R., Matsuoka, Y., 1980. Duck influenza lacking evidence of disease signs and immune response. Infect. Immun. 30, 547–553.

Kim, J.K., Negovetich, N.J., Forrest, H.L., Webster, R.G., 2009. Ducks: the "Trojan horses" of H5N1 influenza. Influenza Other Respi Viruses 3, 121–128.

Kim, J.K., Seiler, P., Forrest, H.L., Khalenkov, A.M., Franks, J., Kumar, M., Karesh, W.B., Gilbert, M., Sodnomdarjaa, R., Douangngeun, B., Govorkova, E.A., Webster, R.G., 2008. Pathogenicity and vaccine efficacy of different clades of Asian H5N1 avian influenza A viruses in domestic ducks. J. Virol. 82, 11374–11382.

Kishida, N., Sakoda, Y., Isoda, N., Matsuda, K., Eto, M., Sunaga, Y., Umemura, T., Kida, H., 2005. Pathogenicity of H5 influenza viruses for ducks. Arch. Virol. 150, 1383–1392.

Kou, Z., Li, Y., Yin, Z., Guo, S., Wang, M., Gao, X., Li, P., Tang, L., Jiang, P., Luo, Z., Xin, Z., Ding, C., He, Y., Ren, Z., Cui, P., Zhao, H., Zhang, Z., Tang, S., Yan, B., Lei, F., Li, T., 2009. The survey of H5N1 flu virus in wild birds in 14 Provinces of China from 2004 to 2007. PLoS ONE 4, e6926.

L'Vov, D.K., Zhchelkanov, M., Vlasov, N.A., Prilipov, A.G., Deriabin, P.G., Fediakina, I.T., Galkina, I.V., Zaberezhnyi, A.D., Liapina, O.V., Shliapnikova, O.V., Kireev, D.E., Fesenko, E.E., Kalmykov, M.V., Vitkova, O.N., Morozova, T.N., Proshina, E.S., Grebennikova, T.V., Akanina, D.S., Samokhvalov, E.I., Al'khovskii, S.V., Volkov, V.A., Semenov, V.I., Gaponov, V.V., Shmakov, N.I., Kushnir, A.T., Kazarian, A.S., Starikov, N.S., Petrenko, M.S., Slavskii, A.A., Litvin, K.E., Shcherbakova, L.O., Frolov, A.V., Manin, T.B., Umanets, O.A., Bandeev, V.V., Khvan, A.M., Dunaev, V.G.,

Cheledina, T.P., Abgarian, S.R., Mikhailovich, V.M., Zasedatelev, A.S., Liubchenko, E.N., Fliagin, V.N., Tikhonova, I.F., Maslov, D.V., Anan'ev, V., Baranov, N.I., Gorelikov, V.N., Iakovlev, S.S., Aliper, T.I., Nepoklonov, E.A., Suarez, D., 2008. The first break-through of the genotype 2.3.2 of high-virulence influenza A virus A/H5N1, which is new for Russia, in the Far East. Vopr. Virusol. 53, 4–8.

Li, K.S., Guan, Y., Wang, J., Smith, G.J., Xu, K.M., Duan, L., Rahardjo, A.P., Puthavathana, P., Buranathai, C., Nguyen, T.D., Estoepangestie, A.T., Chaisingh, A., Auewarakul, P., Long, H.T., Hanh, N.T., Webby, R.J., Poon, L.L., Chen, H., Shortridge, K.F., Yuen, K.Y., Webster, R.G., Peiris, J.S., 2004. Genesis of a highly pathogenic and potentially pandemic H5N1 influenza virus in eastern Asia. Nature 430, 209–213.

Lipatov, A.S., Kwon, Y.K., Sarmento, L.V., Lager, K.M., Spackman, E., Suarez, D.L., Swayne, D.E., 2008. Domestic pigs have low susceptibility to H5N1 highly pathogenic avian influenza viruses. PLoS Path. 4, e1000102.

Monne, I., Fusaro, A., Al-Blowi, M.H., Ismail, M.M., Khan, O.A., Dauphin, G., Tripodi, A., Salviato, A., Marangon, S., Capua, I., Cattoli, G., 2008. Co-circulation of two sublineages of HPAI H5N1 virus in the Kingdom of Saudi Arabia with unique molecular signatures suggesting separate introductions into the commercial poultry and falconry sectors. J. Gen. Virol. 89, 2691–2697.

OIE. 2009a. Manual of Diagnostic Tests and Vaccines for Terrestrial Animals 2009 "Avian Influenza". http://www.oie.int/eng/normes/mmanual/A_summry.htm.

OIE, 2009b. Weekly Disease Information. http://www.oie.int/wahis/public.php?page=weekly_report_index&admin=0.

Okazaki, K., Takada, A., Ito, T., Imai, M., Takakuwa, H., Hatta, M., Ozaki, H., Tanizaki, T., Nagano, T., Ninomiya, A., Demenev, V.A., Tyaptirganov, M.M., Karatayeva, T.D., Yamnikova, S.S., Lvov, D.K., Kida, H., 2000. Precursor genes of future pandemic influenza viruses are perpetuated in ducks nesting in Siberia. Arch. Virol. 145, 885–893.

Pantin-Jackwood, M.J., Suarez, D.L., Spackman, E., Swayne, D.E., 2007. Age at infection affects the pathogenicity of Asian highly pathogenic avian influenza H5N1 viruses in ducks. Virus Res. 130, 151–161.

Peiris, J.S., de Jong, M.D., Guan, Y., 2007. Avian influenza virus (H5N1): a threat to human health. Clin. Microbiol. Rev. 20, 243–267.

Pfeiffer, J., Pantin-Jackwood, M., To, T.L., Nguyen, T., Suarez, D.L., 2009. Phylogenetic and biological characterization of highly pathogenic H5N1 avian influenza viruses (Vietnam 2005) in chickens and ducks. Virus Res. 142, 108–120.

Reed, M.L., Bridges, O.A., Seiler, P., Kim, J.K., Yen, H.L., Salomon, R., Govorkova, E.A., Webster, R.G., Russell, C.J., 2010. The pH of activation of the hemagglutinin protein regulates H5N1 influenza virus pathogenicity and transmissibility in ducks. J. Virol. 84, 1527–1535.

Roberton, S.I., Bell, D.J., Smith, G.J., Nicholls, J.M., Chan, K.H., Nguyen, D.T., Tran, P.Q., Streicher, U., Poon, L.L., Chen, H., Horby, P., Guardo, M., Guan, Y., Peiris, J.S., 2006. Avian influenza H5N1 in viverrids: implications for wildlife health and conservation. Proc. Biol. Sci. 273, 1729–1732.

Saitou, N., Nei, M., 1987. The neighbor-joining method: a new method for reconstructing phylogenetic trees. Mol. Biol. Evol. 4, 406–425.

Salzberg, S.L., Kingsford, C., Cattoli, G., Spiro, D.J., Janies, D.A., Aly, M.M., Brown, I.H., Couacy-Hymann, E., De Mia, G.M., Dung do, H., Guercio, A., Joannis, T., Maken Ali, A.S., Osmani, A., Padalino, I., Saad, M.D., Savic, V., Sengamalay, N.A., Yingst, S., Zaborsky, J., Zorman-Rojs, O., Ghedin, E., Capua, I., 2007. Genome analysis linking recent European and African influenza (H5N1) viruses. Emerg. Infect. Dis. 13, 713–718.

Smith, G.J., Fan, X.H., Wang, J., Li, K.S., Qin, K., Zhang, J.X., Vijaykrishna, D., Cheung, C.L., Huang, K., Rayner, J.M., Peiris, J.S., Chen, H., Webster, R.G., Guan, Y., 2006. Emergence and predominance of an H5N1 influenza variant in China. Proc. Natl Acad. Sci. USA 103, 16936–16941.

Smith, G.J., Vijaykrishna, D., Ellis, T.M., Dyrting, K.C., Leung, Y.H., Bahl, J., Wong, C.W., Kai, H., Chow, M.K., Duan, L., Chan, A.S., Zhang, L.J., Chen, H., Luk, G.S., Peiris, J.S., Guan, Y., 2009. Characterization of avian influenza viruses A (H5N1) from wild birds, Hong Kong, 2004-2008. Emerg. Infect. Dis. 15, 402–407.

Soda, K., Ozaki, H., Sakoda, Y., Isoda, N., Haraguchi, Y., Sakabe, S., Kuboki, N., Kishida, N., Takada, A., Kida, H., 2008. Antigenic and genetic analysis of H5 influenza viruses isolated from water birds for the purpose of vaccine use. Arch. Virol. 153, 2041–2048.

Starick, E., Beer, M., Hoffmann, B., Staubach, C., Werner, O., Globig, A., Strebelow, G., Grund, C., Durban, M., Conraths, F.J., Mettenleiter, T., Harder, T., 2008. Phylogenetic analyses of highly pathogenic avian influenza virus isolates from Germany in 2006 and 2007 suggest at least three separate introductions of H5N1 virus. Vet. Microbiol. 128, 243–252.

Sturm-Ramirez, K.M., Hulse-Post, D.J., Govorkova, E.A., Humberd, J., Seiler, P., Puthavathana, P., Buranathai, C., Nguyen, T.D., Chaisingh, A., Long, H.T., Naipospos, T.S., Chen, H., Ellis, T.M., Guan, Y., Peiris, J.S., Webster, R.G., 2005. Are ducks contributing to the endemicity of highly pathogenic H5N1 influenza virus in Asia? J. Virol. 79, 11269–11279.

Takano, R., Nidom, C.A., Kiso, M., Muramoto, Y., Yamada, S., Shinya, K., Sakai-Tagawa, Y., Kawaoka, Y., 2009. A comparison of the pathogenicity of avian and swine H5N1 influenza viruses in Indonesia. Arch. Virol. 154, 677–681.

Uchida, Y., Mase, M., Yoneda, K., Kimura, A., Obara, T., Kumagai, S., Saito, T., Yamamoto, Y., Nakamura, K., Tsukamoto, K., Yamaguchi, S., 2008. Highly pathogenic avian influenza virus (H5N1) isolated from whooper swans. Jpn. Emerg. Infect. Dis. 14, 1427–1429.

Webster, R.G., Yakhno, M., Hinshaw, V.S., Bean, W.J., Murti, K.G., 1978. Intestinal influenza: replication and characterization of influenza viruses in ducks. Virology 84, 268–278.

WHO/OIE/FAO H5N1 Evolution Working Group, 2009. Continuing progress towards a unified nomenclature for the highly pathogenic H5N1 avian influenza viruses: divergence of clade 2.2 viruses. Influenza Other Respir. Viruses 3, 59–62.

Xu, X., Subbarao, K., Cox, N.J., Guo, Y., 1999. Genetic characterization of the pathogenic influenza A/Goose/Guangdong/1/96 (H5N1) virus: similarity of its hemagglutinin gene to those of H5N1 viruses from the 1997 outbreaks in Hong Kong. Virology 261, 15–19.

Journal of NeuroVirology, 16: 125-132, 2010
© 2010 Journal of NeuroVirology
ISSN 1355-0284 print/ 1538-2443 online
DOI: 10.3109/13550281003682521

informa
healthcare

Lipopolysaccharide treatment and inoculation of influenza A virus results in influenza virus–associated encephalopathy–like changes in neonatal mice

Tomohisa Tanaka,[1] Yuji Sunden,[1] Yoshihiro Sakoda,[2] Hiroshi Kida,[2] Kenji Ochiai,[1] and Takashi Umemura[1]

[1]*Laboratorie of Comparative Pathology; and* [2]*Laboratory of Microbiology, Graduate School of Veterinary Medicine, Hokkaido University, Sapporo, Japan*

Influenza virus–associated encephalopathy (IAE) is a highly mortal neural complication of influenza A virus (IAV) infection, mostly affecting children younger than 5 years old, and the brain pathology of IAE is characterized by peracute brain edema with evidence of an impaired blood-brain barrier. The pathogenesis of IAE is unknown, but hypercytokinemia of tumor necrosis factor (TNF)-α, interleukin (IL)-1β, and IL-6 is suspected of playing a central role in the development of IAE. Because the brain pathology of IAE is similar to that of septic encephalopathy due to endotoxemia, the effect of combined treatment of IAV and lipopolysaccharide (LPS) was tested using suckling mice. The results show that pulmonary infection with non-neurotropic IAV enhanced the neuropathogenicity of LPS and induced encephalopathy that was similar to IAE with respect to the occurrence of central nervous system (CNS) histopathology and the absence of direct infection of IAV in the brain. Influenza A virus also increased blood-brain barrier (BBB) permeability and induced inflammatory cytokines in the blood. These results suggested that the mice treated with IAV+LPS are possible animal models of IAE, and that hypercytokinemia and/or the involvement of endotoxemia in IAV infection are possible causes of IAE. *Journal of NeuroVirology* (2010) **16,** 125–132.

Keywords: encephalopathy; inflammatory cytokines; influenza virus; mouse model

Introduction

Influenza virus-associated encephalopathy (IAE) is a rare but highly mortal neural complication of influenza virus infection, mostly affecting children younger than 5 years old (Morishima *et al*, 2002). It has been reported around the world (Toovey, 2008), but patients have been found most frequently in Japan. According to etiological research, IAE is typically associated with non-neurotropic H3N2 influenza A virus (IAV) infection (Morishima *et al*, 2002). Postmortem microscopic analyses on the patients demonstrated hyalinization of blood vessels and extravascular leakage of plasma proteins in the brains, which suggest the occurrence of vasogenic edema due to damage of vascular endothelial cells (Morishima *et al*, 2002). The encephalopathy is often followed by disseminated intravascular coagulation and multiple organ failure (Togashi *et al*, 2004; Yokota *et al*, 2000).

The pathological mechanism of the IAE is unknown. In IAE patients, IAV infects mucosal epithelial cells of the respiratory tract, and an isolation of the virus from the central nervous system (CNS), including the cerebrospinal fluid (CSF), is usually negative (Ito *et al*, 1999; Smidt *et al*, 2004). Therefore, the direct invasion of the virus into the CNS is irrelevant as the cause of IAE. Miniplasmin, a hemagglutinin processing protease, accumulates in the cerebral capillaries of mice with abnormal

Address correspondence to Takashi Umemura, Laboratory of Comparative Pathology, Graduate School of Veterinary Medicine, Hokkaido University, N18 W9, Kita-ku, Sapporo 060-0818, Japan. E-mail: umemura@vetmed.hokudai.ac.jp.
This study was supported by Grants-in-Aid for Scientific Research from the Ministry of Education, Culture, Sports, Science, and Technology, Japan.
Received 6 October 2009; revised 26 November 2009; accepted 8 January 2010.

mitochondrial β-oxidation after non-neurotropic IAV infection (Yao *et al*, 2004). The accumulation of miniplasmin allows non-neurotropic IAV to infect the cerebral vascular endothelial cells, which triggers the increased permeability of the blood-brain barrier (BBB). However, it may not be the cause of IAE, since IAV has not usually been demonstrated in the CNS of IAE patients and this animal model is accompanied by a fatty change in hepatocytes similar to Reyes' syndrome (Okita *et al*, 1996). Elevated concentrations of several cytokines, including tumor necrosis factor (TNF)-α, soluble TNF receptor 1, interleukin (IL)-6, and IL-1β, have been reported in the serum and CSF of IAE patients (Ichiyama *et al*, 2003; Ito *et al*, 1999), and the concentrations of these inflammatory cytokines were correlated with the severity of CNS dysfunction (Aiba *et al*, 2001; Toovey, 2008). From these results, hypercytokinemia is suspected of playing an important role in the development of IAE. However, there are arguments on whether the hypercytokinemia is the cause or result of IAE, since the involvement of hypercytokinemia to IAE has not been experimentally confirmed yet and the direct cause of hypercytokinemia in IAE is unknown.

Sepsis is a condition characterized by uncontrolled bacterial infection and affects many organs, including the CNS. Septic encephalopathy is one of the common complications of sepsis and is characterized by diffuse or multifocal neural dysfunction as a result of an inflammatory response with or without direct bacterial invasion into the brain (Papadopoulos *et al*, 2000). Administration of lipopolysaccharide (LPS), a structural component of the outer membrane of gram-negative bacteria, induces pathological changes that mimic the process of sepsis (Alexander *et al*, 2008; Papadopoulos *et al*, 2000). The predominant microscopic findings of the encephalopathy are vasogenic cerebral edema and neuronal damage (Bogdanski *et al*, 2000; Stolp *et al*, 2005). Although the mechanism of septic encephalopathy is not fully elucidated, TNF might play an important role in the pathogenicity (Alexander *et al*, 2008). Therefore, septic encephalopathy is similar to IAE regarding the involvement of inflammatory cytokines as well as the CNS histopathology.

In this study, we demonstrate that pulmonary infection of non-neurotropic IAV enhances neuropathogenicity of LPS and induces encephalopathy similar to IAE in regards to the occurrence of CNS histopathology with the absence of direct infection of IAV in the brain, an increase of BBB permeability, and the induction of inflammatory cytokines in the blood.

Results

General statuses and survival rates of each group of mice

We gave inoculations of IAV, LPS, or both (IAV+LPS) to 1-week-old ICR mice. The mice of the IAV group showed depression, rough fur, and emaciation at 3 to 4 days post infection (dpi), which progressively worsened. Meanwhile, LPS and IAV+LPS group mice showed similar symptoms as well as diarrhea and a sluggish response to manual stimulations within several hours of the LPS inoculations. The general symptoms appeared severer in the IAV+LPS group than in the LPS group. All the mice in the LPS group survived, whereas 93% and 68% of mice in the IAV and IAV +LPS groups survived, respectively (Figure 1).

Histopathological changes in mice

The mice of the IAV and IAV+LPS groups showed multifocal bronchointerstitial pneumonia in the lungs (Figure 2A). The lesions were mainly located around the bronchioles, and the bronchiolar and alveolar walls were thickened by infiltration of mononuclear cells and neutrophils. Bronchiolar lumina and alveoli also contained a small number of sloughed epithelial cells. There were no obvious differences between the mice in the IAV and IAV +LPS groups regarding the quality, distribution, and severity of the pulmonary lesions. Although there were no any significant lesions in the brains of the IAV group, multifocal microbleeding, irregular dilation of perivascular spaces, and neutrophilic infiltration were found in the brains of the mice in the LPS and IAV+LPS groups (Figure 2B, C). These brain lesions were usually located at the cerebral cortex and brain stem, and were sometimes accompanied by mild spongiform change of neuropils and Alzheimer type 2–like degenerated astrocytes (Figure 2D). These cerebral lesions appeared 24 h after the second inoculation of LPS, and were more prominent in the IAV+LPS group than the LPS group 48 h after this inoculation. Other organs were unremarkable, except that there was a depletion of thymic lymphocytes in the LPS and IAV+LPS groups. There were no significant differences in the histopathological semiquantitative scores on thymic lymphocytic depletion and bronchointerstitial pneumonia between IAV and IAV +LPS groups. Cerebral lesions in the IAV+LPS group were more severe than those in the LPS group,

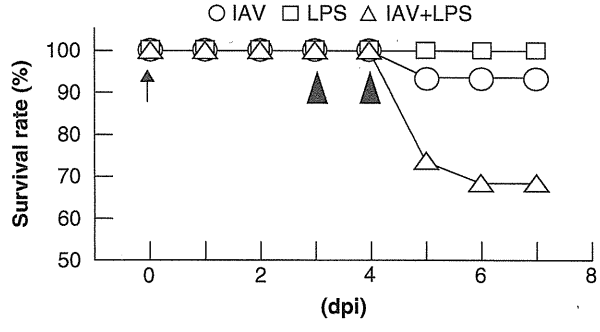

Figure 1 Survival rates of IAV, LPS, and IAV+LPS group mice. The mice were inoculated with IAV (IAV and IAV+LPS groups) or saline (LPS group) at 0 dpi (arrow). Then, the mice received inoculations of LPS (LPS and IAV+LPS mice) or saline (IAV mice) at 3 and 4 dpi (arrow heads).

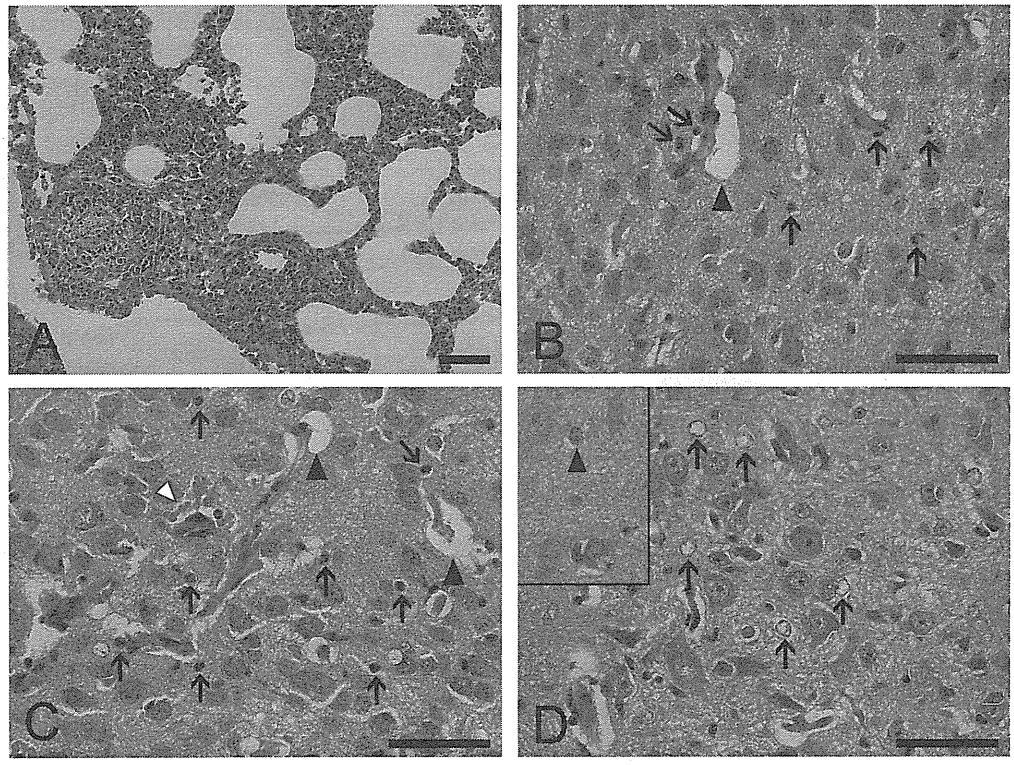

Figure 2 Representative histopathology of the lungs (**A**) and brain (B-D) from IAV+LPS group mice at 5 dpi. (A) Bronchointerstitial pneumonia due to IAV infection. (**B**) Cerebral microbleeding (arrowhead) and irregular dilation of perivascular spaces (arrows). (**C**) Neutrophils (arrows) infiltrating the cerebral cortex. (**D**) Mild spongiform change of neurophil and degenerated astrocytes having vacuolated and swollen nuclei. Hematoxylin and eosin stain. Bars = 50 μm.

especially regarding the severity of cerebral microbleeding (Table 1).

The estimation of cerebrovascular permeability

To evaluate cerebrovascular permeability, we administered Evans blue (EB) dye to the abdominal cavity of mice, and then compared the concentration of the dye in the brains from the IAV, LPS, and IAV+LPS groups. Taken as a whole, the color of the brains from the IAV group was normal, whereas the brains from the LPS and IAV+LPS groups had a noticeable bluish tinge that appeared deeper in the IAV+LPS group than in the LPS group (Figure 3A). To quantify the concentrations of EB dye, the densities of the dye in the brains were measured by absorption spectrometry (Figure 3B). The brains from the IAV+LPS group contained significantly higher levels of the dye than those from the LPS group. These results suggest that the integrity of the BBB significantly deteriorated in the IAV+LPS group, and the results were consistent with histopathological data in which the mice of the IAV+LPS group showed severer cerebral lesions than the other groups.

The induction of cytokines in plasma

In previous studies, it has been reported that the infection of IAV enhanced the inductions of inflammatory cytokines in human leukocytes (Lundemose *et al*, 1993; Nain *et al*, 1990), and inflammatory cytokines were demonstrated to have important roles

Table 1 Scores of microscopic changes

Groups	Time since 2nd LPS injections	Thymus Lymphocytic depletion	Lungs Interstitial pneumonia	Brain		
				Microbleeding	Neutrophilic infiltration	Edema
IAV		0 (0–0)[a]	2 (2–2)	0 (0–0)	0 (0–0)	0 (0–0)
LPS	48 h	2 (1.25–2)	0 (0–0)	1.5 (1–2)	2.5 (1.25–3)	2 (1.25–2)
	72 h	2 (2–2)	0 (0–0)	0 (0–0)	2 (1.5–2)	2 (0.5–2)
IAV+LPS	48 h	3 (3–3)	1.5 (1–2)	3 (3–3)*	3 (3–3)	2 (2–3)
	72 h	2 (1.5–2)	2 (2–2)	0 (0–0)	2 (1.5–2)	1 (1–1.5)

[a]Values mean median of scores (25–75 percentile) in this order. 0 = no obvious change; 1 = focal mild change; 2 = multifocal moderate change; 3 = diffuse, moderate to severe change. *$P < .05$. Differences were analyzed using Mann-Whitney U test.

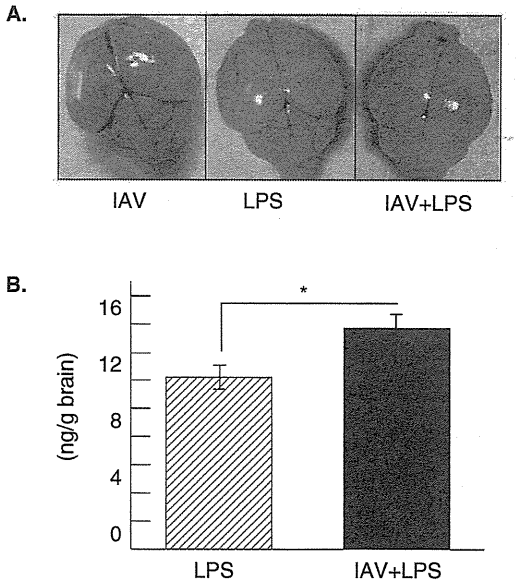

Figure 3 Comparison of BBB integrity. (**A**) Photographs of the brains from the IAV, LPS, and IAV+LPS groups injected intraperitoneally with EB dye. The brains were collected after 48 h of LPS inoculations. (**B**) Quantification of EB dye extracted from the brains. Each error bar means standard error. The statistical comparison was performed using Student's *t* test (*$P < .05$).

as pathogenic agents of LPS (Alexander *et al*, 2008; Papadopoulos *et al*, 2000). Therefore, we measured the levels of plasma cytokines in order to clarify whether IAV infection affects the inductions of inflammatory cytokines by LPS as well as the severity of the encephalopathy. Cytokine levels in the plasma of each group were measured 6, 12, and 24 h after the LPS inoculations. Six hours after the LPS inoculations, the induction of most inflammatory cytokines was upgraded in the LPS and IAV +LPS groups (Figure 4A–D). The serum concentrations of TNF-α and IL-6 in the IAV+LPS group were significantly higher than those in the IAV and LPS groups (Figure 4A, C). In addition, the concentrations of monocyte chemoattractant protein (MCP)-1 and IL-10 in the IAV+LPS group were significantly higher than those in the IAV group (Figure 4B, D). In contrast, the interferon (IFN)-γ level of the IAV group tended to be higher without statistical significance than those of the other groups (Figure 4E). The high cytokine levels in the LPS and IAV+LPS groups dropped to normal or to lower levels than normal until 24 h after of the LPS stimulations (data not shown). Serum concentrations of IL-12p70 were unchanged in all groups throughout the experiments (data not shown).

The distribution of viral antigens and viral titer measurement

Viral antigens were detected by immunohistochemistry in the lungs from IAV and IAV+LPS groups. The IAV antigens were located in bronchiolar epithelial cells and alveolar epithelial cells (Figure 5A). In the bronchioli, many bronchiolar epithelial cells showed positive reaction along the walls, and alveolar

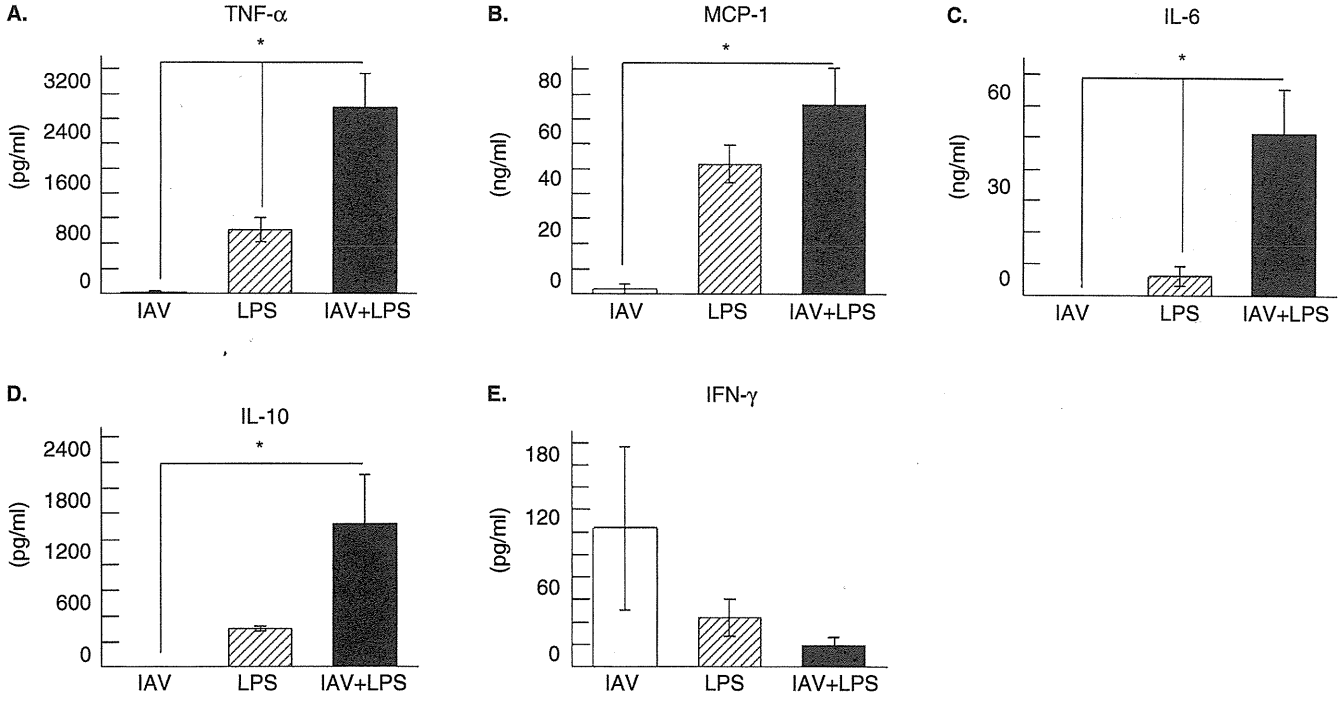

Figure 4 Quantitative analysis of the production of TNF-α (**A**), MCP-1 (**B**), IL-6 (**C**), IL-10 (**D**), and IFN-γ (**E**) in plasma from the IAV, LPS, and IAV+LPS groups. The plasma was collected after 6 h of LPS (or saline) inoculations. Each error bar means standard error. Differences among means were statistically analyzed using Tukey-Kramer multiple comparison tests (*$P < .01$).

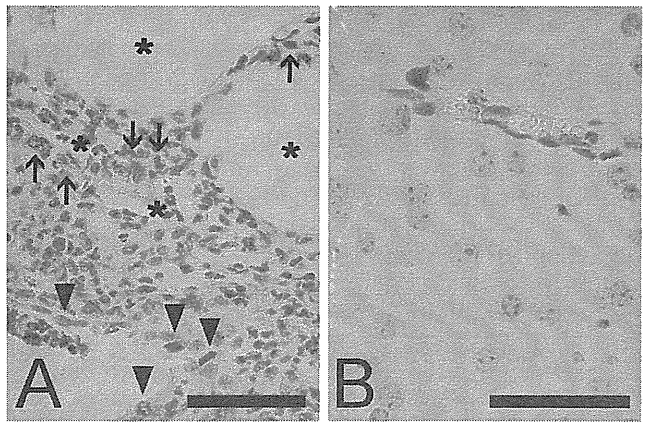

Figure 5 Representative photographs of immunohistochemistry for IAV antigens. (**A**) In the lung from the IAV+LPS group mouse, some bronchiolar and alveolar epithelial cells show positive reactions (arrows). (**B**) The brain of the IAV+LPS mouse is entirely negative for virus antigen. The tissues were collected at 5 dpi of LPS. Bars = 50 μm.

epithelial cells which had oval or flattened shapes showed positive reaction in some thickened alveolar walls. There were no obvious differences in the localization and amounts of the antigen between both groups. However, organs such as the liver, spleen, kidneys, heart, and brain (Figure 5B) stained negative for IAV antigens in the IAV and IAV+LPS groups. We measured viral titers of the lungs and brain by plaque assay. Viral titers in the lungs of the IAV and IAV+LPS groups were 6.62 ± 0.08 and 6.42 ± 0.13 (mean ± SEM: $\log_{10}$ plaque-forming units [PFU]/g), respectively. IAV was not isolated from brain of the IAV and IAV+LPS groups by plaque assay.

Discussion

Early diagnosis, prevention, and therapy for IAE are still to be established because the pathological mechanisms of the disease are unknown. The disease usually occurs in children younger than 5 years of age, and we used neonatal mice to produce IAE in the present experiment. IAV infection induced bronchointerstitial pneumonia in neonatal mice with survival rate of 93% in the IAV group. There were no differences in the viral titers and localization of viral antigen between the IAV and IAV+LPS groups. Survival rates of the IAV+LPS and LPS groups were 68% and 100%, respectively, and only the CNS involvement was severer in the IAV +LPS group than the LPS group. Therefore, the CNS damage was considered to be the direct cause of the decreased survival rate in the IAV+LPS group.

The microscopic cerebral lesions, including microbleeding and dilation of perivascular space, suggest the impairment of cerebral blood vessels and vasogenic edema. This was consistent with the findings of LPS-induced encephalopathy in previous reports (Bogdanski *et al*, 2000; Stolp *et al*, 2005). Scattered neutrophilic infiltration was likely to be the secondary reaction to the brain damage. In our experiment, IAV infection aggravated LPS-induced encephalopathy. Similarly, an infection of infant ferrets with IAV enhanced their susceptibility to the lethal effects of endotoxin (Jakeman *et al*, 1991). The pathological mechanism of LPS encephalopathy remains to be elucidated, but previous studies reported the participation of multiple factors, including inflammatory cells and their mediators, reduced cerebral blood flow, and disruption of the BBB (Papadopoulos *et al*, 2000). In the present study, we did not find any intravascular thrombi in all mice and it was unlikely that microvascular infarction caused cerebral damage in the LPS and IAV+LPS groups. On the other hand, IAV infection enhanced an increase of BBB permeability and the production of TNF-α and IL-6 in plasma of the IAV+LPS mice. The enhanced TNF-α induction may contribute to cerebral vascular damage because TNF-α has a critical role as a pathogenic agent of LPS-induced encephalopathy (Alexander *et al*, 2008). Previous *in vitro* studies using human peripheral blood leukocytes revealed that the production of TNF-α, IL-1, and IL-6 was enhanced by the combined treatment of IAV and LPS (Lundemose *et al*, 1993; Nain *et al*, 1990). Although the mechanism of cytokine induction by IAV and LPS treatment was not elucidated completely, it was suggested that IAV and LPS concurrently activate several common transcription factors responsible for cytokine gene expression, including nuclear factor (NF)-κB, interferon regulatory factor (IRF), and activator protein (AP)-1 (Julkunen *et al*, 2000; Kawai and Akira, 2006). Additionally, LPS is thought to potentiate cytokine synthesis at the posttranscriptional level (Han *et al*, 1990; Nain *et al*, 1990). In the present experiment, the level of plasma TNF-α and the severity of brain lesions were positively correlated. Therefore, the infection of neonatal mice with non-neurotropic IAV might enhance LPS-induced encephalopathy by means of overinduction of cytokines such as TNF-α and IL-6, which contributed to cerebral vascular damage and increased permeability of BBB.

Pathological entity of IAE is vasogenic brain edema due to the damage of vascular endothelial cells without direct invasion of IAV to the brain (Morishima *et al*, 2002). Elevated concentrations of cytokines such as TNF-α and IL-6 may be the cause of the disease (Aiba *et al*, 2001; Ichiyama *et al*, 2003; Ito *et al*, 1999; Toovey, 2008). In the present experiment, IAV+LPS mice showed the IAE-like encephalopathy in respect to the vasogenic brain disorders and the dynamics of plasma inflammatory cytokines without direct infection of IAV to the brain. From these results, it may be concluded that the mice treated with IAV+LPS are a potential animal model of IAE, and that hypercytokinemia and/or the involvement of endotoxemia in IAV infection are possible causes of IAE.

Materials and methods

Virus and mice

Influenza A virus strain A/Aichi/2/68 (H3N2) was propagated in 10-day-old embryonated chicken eggs at 35°C for 48 h (Isoda *et al*, 2006). The virus-containing allantoic fluid was stored at −80°C and used as the source of virus. The infectivity of the virulent fluid was determined using hamagglutinin assay and plaque assay.

Pregnant ICR mice were purchased from Charles River Laboratories Japan (Kanagawa, Japan). The 7-day-old suckling mice were submitted to the following animal experiment. To minimize the difference between maternal mice, the number of neonatal mice was kept around 12 per female mouse. All animal studies were carried out with the approval of the committee of Laboratory Animal Experimentation, Graduate School of Veterinary Medicine, Hokkaido University, and are consistent with the Association for Assessment and Accreditation of Laboratory Animal Care International standards.

Inoculation of influenza virus and LPS to mice

Seven-day-old mice were anesthetized by isoflurane inhalation and inoculated in both nostrils with 10 μl (1×10^5 PFU) of IAV. Then, the mice were inoculated with LPS of *Esherichia coli* O55:B5 (Sigma, St. Louis, MO, USA) twice. Briefly, the mice received 0.5 μg/g of the first LPS injection to the hindlimb muscle at 3 dpi of the virus inoculation, followed by the second injection of 20 μg/g LPS to the peritoneal cavity 24 h after the first injection. Control mice were inoculated with equivalent volumes of sterile saline in place of IAV or LPS. Each mouse was monitored for 7 days, or was submitted to the collection of whole blood under anesthesia and necropsied during 4 to 7 dpi at 6- or 12-h intervals.

Histopathological analysis and semiquantitative evaluation of microscopic changes

At necropsy, tissue samples from the liver, spleen, kidneys, heart, lungs, thymus, and brain were collected from mice, fixed in 20% neutral-buffered formalin solution, and embedded in paraffin wax. The tissue samples were sectioned at a thickness of 4 μm and stained with hematoxylin-eosin stain for light microscopy. Histopathological changes of thymus, lungs, and brains were semiquantitatively scored from score 0 (absent) to score 3 (severe) on the basis of the distribution and severity. Briefly, we made sections from predetermined areas of thymus, lungs and brain. For the evaluation of pulmonary lesion, we obtained four sections from lungs (two sections from the left lung and two sections from the anterior and caudal lobes of the right lung). For the evaluation of brain lesions, we obtained five sections from brain (from each level of frontal lobe, diencephalon, occipital lobe, brain stem, and medulla oblongata). The criteria for scoring were as follows: 0 = no significant lesion; 1 = localized and very mild lesions; 2 = moderate lesions multifocally distributed on more than half of the sections; 3 = moderate to severe lesions diffusely distributed on almost all sections.

Immunohistochemical detection of viral antigen

Serial sections were stained with the streptavidin-biotin immunoperoxidase complex method using Histofine SAB-PO kit (Nichirei, Tokyo, Japan). To restore antigens, the sections were treated with 0.01 M phosphate-buffered saline (PBS) containing 0.1% trypsin (Becton Dickinson, Mountain View, CA, USA) for 20 min at 37°C. As the primary antibody, a diluted rabbit anti-strain A/Whistling swan/Shimane/499/83 (H5N3) hyperimmuno serum (produced in our laboratory) was applied for approximately 12 h at 4°C (Matsuda *et al*, 2004). The chromogenic reaction was performed by 0.05 M Tris-HCl buffer (pH 7.6) containing 0.02% 3,3′-diaminobenzidinetetrahydrochloride (Dojindo Laboratories, Kumamoto, Japan), 0.005% H_2O_2, and 0.01 M imidazole (Sigma). The sections were counterstained with Mayer's hematoxylin. The primary antibody was replaced by 0.01 M PBS for negative controls.

The evaluation of BBB integrity

The integrity of BBB was evaluated by Evans blue (EB; Kanto Chemical, Tokyo, Japan) extravasations, as described previously (Bigdeli and Khoshbaten, 2008; Fukui *et al*, 2003). Briefly, the mice of the IAV group (n = 3), LPS group (n = 4), and IAV +LPS group (n = 4) were injected intraperitoneally with 50 μl of filtered 2% EB solution in sterile saline after 48 h of the second LPS inoculation. The mice were anesthetized after 2 h of EB injection and the brains were rapidly removed. The EB dye in the brains was extracted with 500 μl formamide for 24 h at 38°C. The amount of EB in the supernatants was measured against 90% formamide solution in saline at 630 nm using a plate reader (Multiscan Ascent; Thermo Labsystems, Franklin, MA, USA). EB levels were expressed as ng/g of brain tissue against a standard curve.

The determination of plasma cytokine concentrations

Whole blood was taken into blood collection tubes containing EDTA (Terumo Medical, Elkton, MD, USA). Supernatant plasma was separated by centrifugation at 3500 × g for 2 min and frozen under −80°C until assayed for cytokines. The analysis of plasma cytokine levels was conducted using a mouse inflammation cytometric bead array kit and a FACSArray bioanalyzer (Becton Dickinson, USA) (Li *et al*, 2007; Morgan *et al*, 2004). The experiment was conducted following manufacturer's instructions. Standard curves were determined for each cytokine

from the range of 20 to 5000 pg/ml. The following cytokines were measured: IL-6, IL-10, MCP-1, IFN-γ, TNF-α, and IL-12p70.

Plaque assay

To evaluate viral titer, we performed a plaque assay as previously described (Tsuda *et al*, 2009). Briefly, Mardin-Darby canine kidney (MDCK) cells were grown in Eagle's minimal essential medium (EMEM; Nissui Pharmaceutical, Tokyo, Japan) supplemented with 10% inactivated fetal bovine serum and 2 mM L-glutamine. Pieces of mouse tissues were homogenized in 10% concentration with EMEM under 4°C. The 10-fold dilutions of the homogenized sample were inoculated to confluent monolayers of MDCK cells and incubated for 1 h at 37°C. The dilutions were removed, and the cells were washed with PBS. Cells were overlaid with EMEM containing 1% Bacto Agar (Becton Dickinson) and 0.0005% acetyl trypsin. After 48 h of inoculation at 37°C, cells were stained with 0.005% neutral red for 12 h and visible plaques were counted.

Declaration of interest: The authors report no conflicts of interest. The authors alone are responsible for the content and writing of the paper.

References

Aiba H, Mochizuki M, Kimura M, Hojo H (2001). Predictive value of serum interleukin-6 level in influenza virus-associated encephalopathy. *Neurology* **57:** 295–299.

Alexander J, Jacob A, Cunningham P, Hensley L, Quigg R (2008). TNF is a key mediator of septic encephalopathy acting through its receptor, TNF receptor-1. *Neurochem Int* **52:** 447–456.

Bigdeli M, Khoshbaten A (2008). In vivo preconditioning with normobaric hyperoxia induces ischemic tolerance partly by triggering tumor necrosis factor-alpha converting enzyme/tumor necrosis factor-alpha/nuclear factor-kappaB. *Neuroscience* **153:** 671–678.

Bogdanski R, Blobner M, Becker I, Hänel F, Fink H, Kochs E (2000). Cerebral histopathology following portal venous infusion of bacteria in a chronic porcine model. *Anesthesiology* **93:** 793–804.

Fukui S, Fazzina G, Amorini AM, Dunbar JG, Marmarou A (2003). Differential effects of atrial natriuretic peptide on the brain water and sodium after experimental cortical contusion in the rat. *J Cerebr Bood F Met* **23:** 1212–1218.

Han J, Brown T, Beutler B (1990). Endotoxin-responsive sequences control cachectin/tumor necrosis factor biosynthesis at the translational level. *J Exp Med* **171:** 465–475.

Ichiyama T, Isumi H, Ozawa H, Matsubara T, Morishima T, Furukawa S (2003). Cerebrospinal fluid and serum levels of cytokines and soluble tumor necrosis factor receptor in influenza virus-associated encephalopathy. *Scand J Infect Dis* **35:** 59–61.

Işoda N, Sakoda Y, Kishida N, Bai G, Matsuda K, Umemura T, Kida H (2006). Pathogenicity of a highly pathogenic avian influenza virus, A/chicken/Yamaguchi/7/04 (H5N1) in different species of birds and mammals. *Arch Virol* **151:** 1267–1279.

Ito Y, Ichiyama T, Kimura H, Shibata M, Ishiwada N, Kuroki H, Furukawa S, Morishima T (1999). Detection of influenza virus RNA by reverse transcription-PCR and proinflammatory cytokines in influenza-virus-associated encephalopathy. *J Med Virol* **58:** 420–425.

Jakeman K, Rushton D, Smith H, Sweet C (1991). Exacerbation of bacterial toxicity to infant ferrets by influenza virus: possible role in sudden infant death syndrome. *J Infect Dis* **163:** 35–40.

Julkunen I, Melén K, Nyqvist M, Pirhonen J, Sareneva T, Matikainen S (2000). Inflammatory responses in influenza A virus infection. *Vaccine* **19**(Suppl 1): S32–S37.

Kawai T, Akira S (2006). TLR signaling. *Cell Death Differ* **13:** 816–825.

Li Z, Hulderman T, Salmen R, Chapman R, Leonard S, Young S, Shvedova A, Luster M, Simeonova P (2007). Cardiovascular effects of pulmonary exposure to single-wall carbon nanotubes. *Environ Health Perspect* **115:** 377–382.

Lundemose J, Smith H, Sweet C (1993). Cytokine release from human peripheral blood leucocytes incubated with endotoxin with and without prior infection with influenza virus: relevance to the sudden infant death syndrome. *Int J Exp Pathol* **74:** 291–297.

Matsuda K, Park C, Sunden Y, Kimura T, Ochiai K, Kida H, Umemura T (2004). The vagus nerve is one route of transneural invasion for intranasally inoculated influenza A virus in mice. *Vet Pathol* **41:** 101–107.

Morgan E, Varro R, Sepulveda H, Ember J, Apgar J, Wilson J, Lowe L, Chen R, Shivraj L, Agadir A, Campos R, Ernst D, Gaur A (2004). Cytometric bead array: a multiplexed assay platform with applications in various areas of biology. *Clin Immunol* **110:** 252–266.

Morishima T, Togashi T, Yokota S, Okuno Y, Miyazaki C, Tashiro M, Okabe N, (2002). Encephalitis and encephalopathy associated with an influenza epidemic in Japan. *Clin Infect Dis* **35:** 512–517.

Nain M, Hinder F, Gong J, Schmidt A, Bender A, Sprenger H, Gemsa D (1990). Tumor necrosis factor-alpha production of influenza A virus-infected macrophages and potentiating effect of lipopolysaccharides. *J Immunol* **145:** 1921–1928.

Okita K, Tokino T, Nishimori H, Miura K, Nikaido H, Hayakawa J, Ono A, Kuwajima M, Matsuzawa Y, Nakamura Y (1996). Definition of the locus responsible for systemic carnitine deficiency within a 1.6-cM region of mouse chromosome 11 by detailed linkage analysis. *Genomics* **33:** 289–291.

Papadopoulos M, Davies D, Moss R, Tighe D, Bennett E (2000). Pathophysiology of septic encephalopathy: a review. *Crit Care Med* **28:** 3019–3024.

Smidt MH, Stroink H, Bruinenberg JFM, Peeters M (2004). Encephalopathy associated with influenza A. *Eur J Paediatr Neurol* **8:** 257–260.

Stolp H, Dziegielewska K, Ek C, Habgood M, Lane M, Potter A, Saunders N (2005). Breakdown of the blood-brain barrier to proteins in white matter of the developing brain following systemic inflammation. *Cell Tissue Res* **320:** 369–378.

Togashi T, Matsuzono Y, Narita M, Morishima T (2004). Influenza-associated acute encephalopathy in Japanese children in 1994–2002. *Virus Res* **103:** 75–78.

Toovey S (2008). Influenza-associated central nervous system dysfunction: a literature review. *Travel Med Infect Dis* **6:** 114–124.

Tsuda Y, Isoda N, Sakoda Y, Kida H (2009). Factors responsible for plaque formation of A/duck/Siberia/272/1998 (H13N6) influenza virus on MDCK cells. *Virus Res* **140:** 194–198.

Yao D, Chen Y, Kuwajima M, Shiota M, Kido H (2004). Accumulation of mini-plasmin in the cerebral capillaries causes vascular invasion of the murine brain by a pneumotropic influenza A virus: implications for influenza-associated encephalopathy. *Biol Chem* **385:** 487–492.

Yokota S, Imagawa T, Miyamae T, Ito S, Nakajima S, Nezu A, Mori M (2000). Hypothetical pathophysiology of acute encephalopathy and encephalitis related to influenza virus infection and hypothermia therapy. *Pediatr Int* **42:** 197–203.

This paper was first published online on Early Online on 29 March 2010.

J Med Primatol doi:10.1111/j.1600-0684.2009.00395.x

ORIGINAL ARTICLE

Amelioration of pneumonia with *Streptococcus pneumoniae* infection by inoculation with a vaccine against highly pathogenic avian influenza virus in a non-human primate mixed infection model

Taichiro Miyake[1,2], Kosuke Soda[3], Yasushi Itoh[1], Yoshihiro Sakoda[3], Hirohito Ishigaki[1], Tomoya Nagata[1,4], Hideaki Ishida[1], Misako Nakayama[1], Hiroichi Ozaki[5], Hideaki Tsuchiya[6], Ryuzo Torii[6], Hiroshi Kida[3,7] & Kazumasa Ogasawara[1]

1 Department of Pathology, Shiga University of Medical Science, Otsu, Shiga, Japan
2 Department of Ophthalmology, Shiga University of Medical Science, Otsu, Shiga, Japan
3 Department of Disease Control, Graduate School of Veterinary Medicine, Hokkaido University, Sapporo, Japan
4 Department of Otorhinolaryngology, Head and Neck Surgery, Shiga University of Medical Science, Otsu, Shiga, Japan
5 Faculty of Agriculture, Tottori University, Tottori, Japan
6 Research Center for Animal Life Science, Shiga University of Medical Science, Otsu, Shiga, Japan
7 Research Center for Zoonosis Control, Hokkaido University, Sapporo, Japan

Keywords
cynomolgus macaque – H7N7 – superinfection

Correspondence
Yasushi Itoh, Department of Pathology, Shiga University of Medical Science, 485 Setatsukinowa, Otsu, Shiga 520-2192, Japan.
Tel.: +81 77 548 2172;
fax: +81 77 548 2423;
e-mail: yasushii@belle.shiga-med.ac.jp

Accepted October 9, 2009.

Abstract

Background Highly pathogenic avian influenza virus (HPAIV) infection has a high mortality rate in humans. Secondary bacterial pneumonia with HPAIV infection has not been reported in human patients, whereas seasonal influenza viruses sometimes enhance bacterial pneumonia, resulting in substantial morbidity and mortality. Therefore, if HPAIV infection were accompanied by bacterial infection, an increase in mortality would be expected. We examined whether a vaccine against HPAIV prevents severe morbidity caused by mixed infection with HPAIV and bacteria.
Methods H7N7 subtype of HPAIV and *Streptococcus pneumoniae* were inoculated into cynomolgus macaques with or without vaccination of inactivated whole virus particles.
Results Vaccination against H7N7 HPAIV decreased morbidity caused by HPAIV and pneumonia caused by *S. pneumoniae*. Bacterial replication in lungs was decreased by vaccination against HPAIV, although the reduction in bacterial colonies was not significant.
Conclusions Vaccination against HPAIV reduces pneumonia caused by bacterial superinfection and may improve prognosis of HPAIV-infected patients.

Introduction

Influenza virus and *Streptococcus pneumoniae* are the two pathogens that cause the majority of respiratory infections in humans. Influenza virus infection results in pneumonitis in which lymphocytes infiltrate into lung interstices, whereas bacteria induce pneumonia in which neutrophils infiltrate into lung alveoli. Although influenza virus infection alone results in pneumonitis, secondary bacterial pneumonia may be a major cause of substantial morbidity and mortality during typical influenza pandemics, including the major pandemic of 1918–1919 [2, 21]. Although bacterial pneumonia has not been reported in patients infected with H5N1 or H7N7 highly pathogenic avian influenza virus (HPAIV) [5, 26], the possibility of mortality being increased by

© 2009 John Wiley & Sons A/S

mixed infection with HPAIV and bacteria has not been ruled out. Thus, it seems reasonable to assume that the prevention of influenza virus replication will improve bacterial pneumonia in case of mixed infection, resulting in decreased morbidity and mortality; however, this assumption has not been examined, at least in macaque models. In this study, as HPAIV A/chicken/Netherlands/2586/2003 (H7N7) (NL2586) was more pathogenic, i.e. duration of high fever and loss of appetite, in cynomolgus macaques than A/Vietnam/1194/2004 (H5N1) [8] (Itoh, Y., *et al.*, unpublished data), we examined the efficacy of inoculation with a vaccine against H7N7 HPAIV for ameliorating bacterial pneumonia in a non-human primate model with mixed infection.

In recent years, results of epidemiological and animal model studies have demonstrated that initial respiratory tract infection alters immunity to a second unrelated pathogen, even long after the resolution of the first pathogen and in the absence of cross-reactive immunity [15, 29]. Several factors have been proposed to be involved in this altered immunity, including suppression of neutrophil function [1, 4, 13] and induction of inhibitory interleukin (IL)-10 [27, 28]. In another study, it was shown that interferon-γ produced by T cells in the lung after viral infection inhibits alveolar macrophage-mediated microbial clearance and, consequently, leads to enhanced susceptibility to secondary bacterial infection [24].

We previously demonstrated that whole virus particle vaccines inactivated by formalin induced protective immune responses, including antibody and cytotoxic T lymphocyte responses, against HPAIV in mice [18]. We selected vaccine strains of non-pathogenic H5N1 and H7N7 viruses, A/duck/Hokkaido/Vac-1/2004 (Vac-1) and A/duck/Hokkaido/Vac-2/2004 (Vac-2) respectively, from a virus library containing 144 different combinations of 16 hemagglutinin (HA) and 9 neuraminidase (NA) subtypes of non-pathogenic viruses [10] and produced whole virus particle vaccines as described previously [17, 20]. Then, we examined immune responses induced by subcutaneous inoculation with the whole virus particle vaccine and protective efficiency against H5N1 and H7N7 HPAIVs in non-human primate models [8] (Itoh, Y., *et al.*, unpublished data). The whole virus particle vaccines ameliorated morbidity including high fever and appetite loss in cynomolgus macaques. HPAIV was detected in samples from unvaccinated macaques for 5–7 days after challenge with HPAIV, whereas HPAIV was recovered from samples of the vaccinated macaques only for 1–2 days after challenge.

In the present study, vaccination with Vac-2 against H7N7 HPAIV decreased histopathological pneumonia caused by *S. pneumoniae* in macaques simultaneously infected with H7N7 HPAIV and *S. pneumoniae*. Bacterial growth in the lung was diminished by vaccination with Vac-2, although the reduction was not significant. Therefore, development of vaccines against influenza virus might be crucial for preventing high rates of morbidity and mortality in pandemics.

Materials and methods

Viruses

Non-pathogenic influenza virus A/duck/Hokkaido/Vac-2/2004 (H7N7) (Vac-2, National Center for Biotechnology Information taxonomy database ID: 390987) is a genetic reassortant generated by co-infection with A/duck/Mongolia/736/2002 (H7N7) and A/duck/Hokkaido/49/1998 (H9N2) in chicken embryos. PB2, PB1, PA, HA, NA and NS genes of Vac-2 were derived from the H7N7 virus, and NP and M genes were derived from the H9N2 virus [17]. HPAIV A/chicken/Netherlands/2586/2003 (H7N7) (NL2586, National Center for Biotechnology Information taxonomy database ID: 533037) was provided by Dr Ilaria Capua [L'Office International des Épizooties (OIE), Food and Agriculture Organization of the United Nations (FAO), and National Reference Laboratory for Newcastle Disease and Avian Influenza, Istituto Zooprofilattico Sperimentale delle Venezie, Italy]. The percent sequence similarity between Vac-2 and NL2586 was 97% in HA and 98% in NA at the amino acid level. The viruses were propagated in the allantoic cavities of 10-day-old embryonated hen's eggs at 35°C for 48 hours. For an inactivated vaccine, the infectious allantoic fluids were concentrated and purified by high-speed centrifugation through a 10–50% sucrose density gradient (112,500 *g* for 90 minutes) and then treated with 0.1% formalin at 4°C for 1 week. The purified viruses were then suspended in PBS. Inactivation of the viruses was confirmed by the absence of detectable hemagglutination following inoculation of the materials into 10-day-old embryonated hen's eggs after one passage [20]. The amount of whole particle vaccines was indicated as that of entire protein including HA and the other viral proteins. The vaccine used in this study contained 42,667 HA units of HA antigen in 1 mg vaccine.

For virus titration, serial dilutions of swabs and whole blood samples were inoculated onto confluent Madin–Darby canine kidney (MDCK) cells. The MDCK cells were then cultured in MEM including 0.1% BSA. Cytopathic effects were examined with a microscope 72 hours later, and mean tissue infectious dose ($TCID_{50}$)/ml was calculated [8].

© 2009 John Wiley & Sons A/S

Bacteria

Streptococcus pneumoniae was obtained from Dr Takayuki Ezaki (Gifu University, GTC261, NCTC7465). The bacteria were stored at −80°C in 10% (w/v) skimmed milk. For preparation of the animal inoculation, 10-μl aliquots of bacteria were removed from frozen stock and inoculated into 40 ml of brain–heart infusion broth (Becton, Dickinson and Company, Sparks, MD, USA) and then incubated at 37°C for 17 hours. Bacteria were collected by centrifugation at 700 *g* for 30 minutes and resuspended in 10 ml saline. A 1-ml aliquot of the saline suspension was used for inoculation into each animal, and the remainder was used for quantification and colony counting by serial dilution [16, 19].

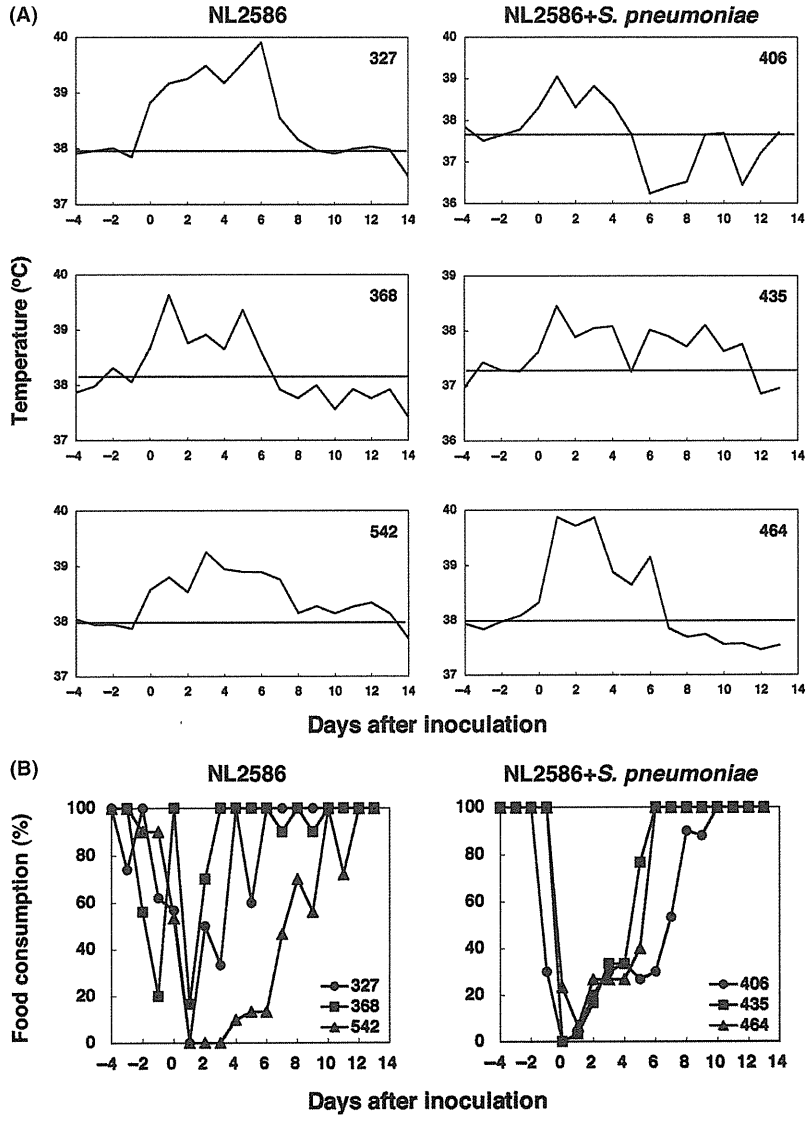

Fig. 1 Body temperatures and food consumption of macaques after inoculation of H7N7 HPAIV (NL2586) with or without *Streptococcus pneumoniae*. NL2586 (4×10^7 $TCID_{50}$) was inoculated onto conjunctivas and into nasal cavities and tracheas with *S. pneumoniae* (1.2×10^9 CFU) into tracheas of cynomolgus macaques (Nos 406, 435 and 464). The other macaques (Nos 327, 368 and 542) were inoculated with NL2586 (4×10^7 $TCID_{50}$) onto conjunctivas and into nasal cavities and tracheas. (A) Body temperatures were monitored by telemetry transmitters implanted in the peritoneal cavities. Average temperatures of the highest and lowest temperatures on one day are time-dependently shown. Lines drawn horizontally indicate the average temperature levels at pre-infection. (B) Appetite was reflected by the amount of food consumed, which was calculated from the numbers of residual and fed pellets.

J Med Primatol **39** (2010) 58–70
© 2009 John Wiley & Sons A/S

Swab samples were collected as described in the following. To count the colony number, swab samples were serially diluted. Diluted fluid was cultured on blood agar plates with 5% sheep blood (Eiken Chemical Co. Ltd, Tokyo, Japan) at 37°C for 21 hours. *Streptococcus pneumoniae* colonies were identified by their hemolytic activity and counted. *Streptococcus pneumoniae* colonies characteristically produce a zone of alpha hemolysis (incomplete, green) on blood agar [16].

Animals

Five- to seven-year-old cynomolgus macaques (*Macaca fascicularis*) from Vietnam were used with permission of the Shiga University of Medical Science Animal Experiment Committee and Biosafety Committee and in accordance with Guidelines for the Husbandry and Management of Laboratory Animals of Research Center for Animal Life Science at Shiga University of Medical Science. In the text and figures, individual macaques are distinguished by identification numbers. The absence of H7N7-specific antibody in the sera was confirmed before experiments using antigen-specific enzyme-linked immunosorbent assays (ELISA). Under anesthesia 2 weeks before virus inoculation, telemetry probes (TA10CTA-D70; Data Sciences International, St Paul, MN, USA) to monitor body temperature were implanted in the macaques' peritoneal cavities. The macaques used in this study did not carry B virus, hepatitis E virus, *Mycobacterium tuberculosis*, *Shigella* spp., *Salmonella* spp. or *Entamoeba histolytica* [8].

The vaccines (1 mg/dose) were inoculated subcutaneously with syringes with alum (500 μl; Superfos Biosector, Vaerloese, Denmark) twice with a 2-week interval between injections. Saline (500 μl) was injected into control animals. Five weeks after the second vaccination, NL2586 (4×10^7 $TCID_{50}$) was inoculated on conjunctivas (1×10^6 $TCID_{50}$/50 μl for each eye) and

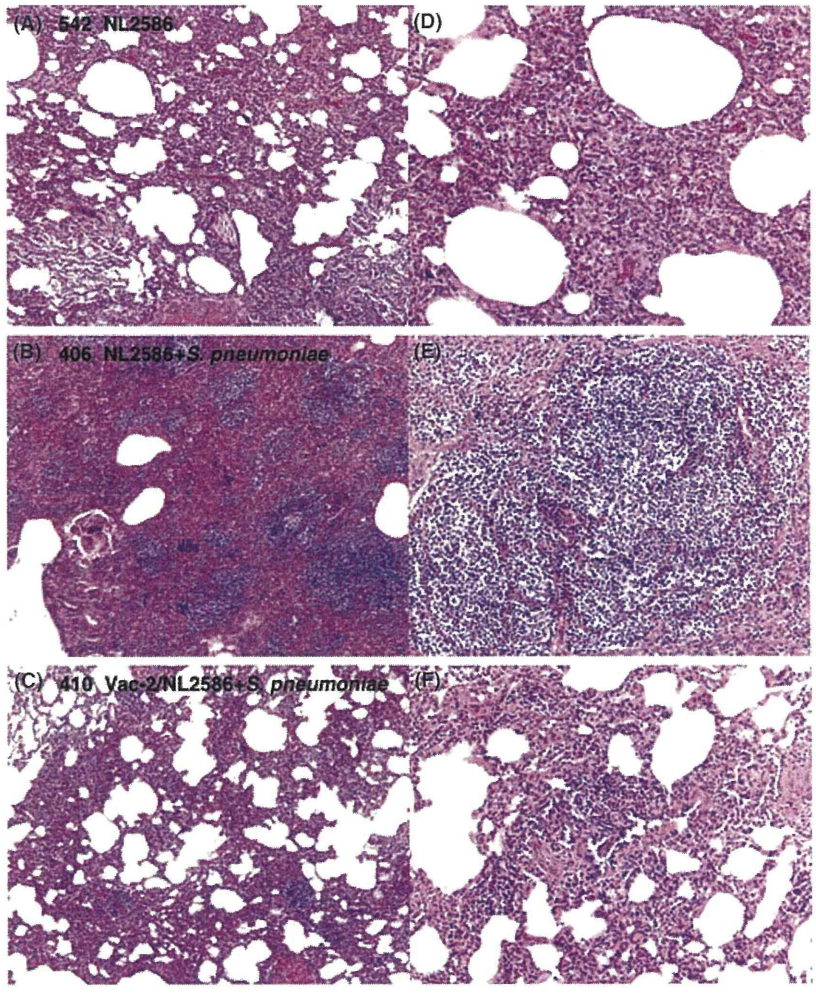

Fig. 2 Lung histology of cynomolgus macaques inoculated with NL2586 with or without *Streptococcus pneumoniae*. Cynomolgus macaques were subcutaneously vaccinated with inactivated whole particles of Vac-2 twice. Seven weeks after the first vaccination (5 weeks after the second vaccination), the macaques were inoculated with pathogens. After autopsy (i.e. 14 days after the challenge), the lungs were fixed in 10% formalin. Hematoxylin and eosin (H&E) staining was conducted as described in Materials and methods. The figures (A–C) show the low power magnification and (D–F) high power magnification. (A, D) An unvaccinated macaque (No. 542) inoculated with NL2586 alone; (B, E) an unvaccinated macaque (No. 406) inoculated with NL2586 and *S. pneumoniae*; (C, F) a vaccinated macaque (No. 410) inoculated with NL2586 and *S. pneumoniae*.

© 2009 John Wiley & Sons A/S

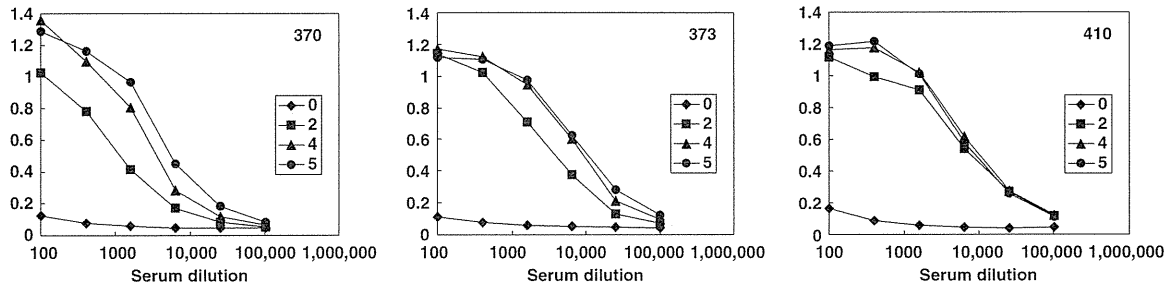

Fig. 3 Antibody responses specific for H7N7 vaccine antigens in cynomolgus macaques immunized with whole virus particle vaccines. Cynomolgus macaques were subcutaneously inoculated with whole virus particle vaccines of Vac-2 (1 mg/dose) with alum twice with a 2-week interval between injections. Sera were collected before (0 week) and after vaccination (2, 4 and 5 weeks after the first vaccination). IgG antibodies specific for Vac-2 antigens in sera were analyzed at indicated dilutions using ELISA. Optical densities at 450 nm are shown.

into nasal cavities (9×10^6 $TCID_{50}$/450 μl for each nasal cavity) with pipettes and into tracheas (2×10^7 $TCID_{50}$/1 ml) with catheters. *Streptococcus pneumoniae* (1.2×10^9 CFU/1 ml) was inoculated into tracheas with catheters. Experiments using NL2586 were performed in the biosafety level 3 facility of the Research Center for Animal Life Science, Shiga University of Medical Science.

Under anesthesia, two cotton sticks were used to collect each swab; subsequently, the sticks were immersed in 1 ml of PBS containing 0.1% BSA. A bronchoscope (MEV-2560; Machida Endoscope Co., Ltd, Tokyo, Japan) and brushes (BC-203D-2006; Olympus, Tokyo, Japan) were used to collect samples of bronchi [25]. The brushes were immersed in 1 ml of PBS containing BSA.

Histological examination

After autopsy, the lungs were fixed in 10% formalin for at least 1 week. Hematoxylin and eosin staining was conducted as previously described [8].

Enzyme-linked immunosorbent assays

The antibody titers of serum samples against Vac-2 antigens were determined using ELISA. Then 96-well plates were coated with 50 μl of purified Vac-2 (20 μg/ml) [8]. For analysis of antibody responses against *S. pneumoniae*, *S. pneumoniae* was cultured as described previously. Thereafter, *S. pneumoniae* was suspended in PBS and inactivated by heat (100°C, 10 minutes). ELISA plates were coated with 50 μl of inactivated *S. pneumoniae* (2×10^5 CFU) [22]. Serially diluted samples were incubated overnight in the coated plates. After washing five times, horseradish peroxidase-conjugated anti-monkey IgG antibody (MP Biomedicals, Inc./Cappel, Aurora, OH, USA) (1:1000 × 50 μl) was added and incubated for 1 hour at room temperature. Horseradish peroxidase activity was assessed using 3, 3′, 5, 5′-tetramethyl benzidine substrate (100 μl). The reaction was stopped by the addition of 1 M hydrogen chloride (100 μl). Optical density was measured at 450 nm.

For detection of IL-10, a monkey IL-10 ELISA kit was used as according to a manufacturer's instruction (Bender MedSystems GmbH, Vienna, Austria). IL-10 secretion was expressed as relative changes comparing with IL-10 production after infection and before infection.

Virus neutralization assay

The serum samples were pretreated with receptor destroying enzyme (RDEII; Denka Seiken, Tokyo, Japan) at 37°C overnight and then inactivated at 56°C for 1 hour. Diluted samples were mixed with 50 $TCID_{50}$ of NL2586 for 1 hour. Then the mixture was added onto an MDCK monolayer. After 1-h incubation, the suspension was removed, and the cells were cultured in MEM containing 0.1% BSA. After incubation at 35°C for 3 days, the number of wells with cytopathic effects was counted in quadruplicate culture. Neutralization titers were expressed as the dilution in which cytopathic effects were observed in 50% of the wells.

Results

Pathogenicity of simultaneous infection with H7N7 HPAIV and Streptococcus pneumoniae in cynomolgus macaques and efficacy of ameliorating pneumonia with Streptococcus pneumoniae by a vaccine against H7N7 HPAIV

H7N7 HPAIV NL2586 (4×10^7 $TCID_{50}$) or both NL2586 and *S. pneumoniae* were inoculated on conjunctivas and in nasal cavities and tracheas of cynomolgus

J Med Primatol **39** (2010) 58–70
© 2009 John Wiley & Sons A/S

Table 1 *Streptococcus pneumoniae* titers in bronchial swabs

		Number of colonies (×10^2 CFU/ml)								
	Animal (dpi)	0	1	2	3	4	5	6	7	8
Without Vac-2	406	0	0	0	0	0	0	0	0	0
	435	0	1	33	2	0	0	0	0	0
	464	0	0	0	0	1	0	0	0	0
With Vac-2	370	0	0	0	0	0	0	0	0	0
	373	0	0	0	0	0	0	0	0	0
	410	0	0	0	0	0	0	0	0	0

Macaques were subcutaneously vaccinated with Vac-2 twice. Five weeks after the second vaccination, the macaques were inoculated with NL2586 and *S. pneumoniae*. Bronchial swabs were collected with a bronchoscope on the indicated days. dpi, days post inoculation with NL2586 and *S. pneumoniae*.

macaques. The body temperature was time-dependently expressed by an average of highest and lowest temperatures on 1 day, and the body temperature after the virus challenge was compared with that before the virus challenge. After NL2586 inoculation, higher body temperature than that before the challenge was observed for 6–13 days in the macaques (Nos 327, 368, 542; Fig. 1A, left panels). After simultaneous inoculation with NL2586 and *S. pneumoniae*, high body temperature was observed until day 4 (No. 406, followed by unstable low temperature until day 12), day 6 (No. 464) and day 11 (No. 435) (Fig. 1A, right panels).

After NL2586 challenge, loss of appetite was observed in two macaques for 2–5 days and in one macaque for 10 days, and after challenge with both NL2586 and *S. pneumoniae*, loss of appetite was observed in two macaques for 6 days and in one macaque for 10 days (Fig. 1B). We also compared weight loss among macaques challenged with the pathogens. All of the macaques had lost weight on day 14 after the virus challenge; the average weight ratio (after/before the challenge) in macaques challenged with NL2586 alone was 90%, whereas that in macaques challenged with NL2586 and *S. pneumoniae* was 88%. These were not significantly different and coincide with the findings for appetite loss ($P = 0.33$).

Next, we performed histological examination of the lungs 14 days after the challenge. The lungs of macaques infected with NL2586 alone indicated interstitial lymphocyte infiltration in thick alveolar walls (pneumonitis) (Fig. 2A,D), whereas pneumonitis and alveolar lymphocyte infiltration with a few neutrophils

Table 2 *Streptococcus pneumoniae* titers in lungs at autopsy

	Number of colonies (×10^2 CFU/ml)					
	Without Vac-2			With Vac-2		
Lung lobe	406	435	464	370	373	410
Upper right	0	1	5	0	4	1
Middle right	0	13	3	1	1	3
Lower right	0	0	6	4	1	2
Upper left	1	0	5	0	0	2
Middle left	0	2	1	1	1	1
Lower left	0	1	1	0	0	2
Total	1	17	21	6	7	11

Lung tissues were collected at autopsy (14 days after inoculation with NL2586 and *S. pneumoniae*). Tissues were homogenized and suspended in PBS to be adjusted to 10% (w/v) solution.

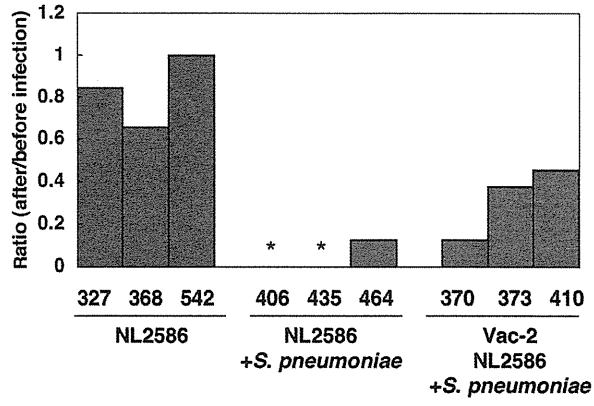

Fig. 4 IL-10 secretions in nasal swab samples. The levels of IL-10 in the samples were analyzed by ELISA. Nasal swabs were collected on day 0 before inoculation and day 8 after inoculation with NL2586 with or without *Streptococcus pneumoniae* as described in Table 3. The levels on day 8 were compared with the day 0 baseline to determine the relative changes in each macaque. Average fold-changes of IL-10 (day 8/day 0) are 0.83, 0.04 and 0.32 in macaques inoculated with NL2586 alone, unvaccinated macaques inoculated with NL2586 and *S. pneumoniae*, and vaccinated macaques inoculated with NL2586 and *S. pneumoniae* respectively, when the concentrations below the detection limit were calculated as 0 unit/ml (*). The differences of IL-10 relative levels are significant in NL2586 alone vs. NL2586 and *S. pneumoniae* ($P = 0.002$) and in NL2586 alone vs. Vac-2 + NL2586 and *S. pneumoniae* ($P = 0.02$).

© 2009 John Wiley & Sons A/S

(pneumonia) was observed in lungs of macaques infected with both NL2586 and *S. pneumoniae* (Fig. 2B,E). It was likely that acute-phase inflammation with neutrophils against *S. pneumoniae* disappeared following lymphocyte infiltration (i.e. tissue-repairing phase) 2 weeks after the simultaneous infection.

The above findings indicated that simultaneous infection resulted in histopathological pneumonitis and pneumonia but did not result in enhanced morbidity in the macaques. Thus, we histologically examined the efficacy of a vaccine, Vac-2, against H7N7 HPAIV for improving the bacterial pneumonia. Macaques were subcutaneously immunized twice with inactivated Vac-2, and subsequent increase in vaccine antigen-specific IgG in sera was confirmed (Fig. 3). Five weeks after the second vaccination, NL2586 and *S. pneumoniae* were inoculated into the macaques. Fourteen days after the challenge, lung tissue was examined at autopsy. The lungs of vaccinated macaques showed slight pneumonitis, but only weak pneumonia was seen in the lungs even after infection with both NL2586 and *S. pneumoniae* (Fig. 2C,F). Thus, we concluded that the vaccine against H7N7 HPAIV prevented severe bacterial pneumonia.

Bacterial growth in the bronchi and lungs of cynomolgus macaques infected with NL2586

We also examined bacterial growth in the bronchi and lungs of macaques simultaneously infected with NL2586 and *S. pneumoniae*. Bacterial colonies were detected in the bronchi of macaques 435 and 464 until day 4 after inoculation (Table 1), whereas bacterial colonies were observed in the lungs of all three macaques on day 14 (Table 2). On the other hand, bacterial colonies were decreased in the lungs of vaccinated macaques compared with those in the non-vaccinated macaques, although the reduction was not significant ($P = 0.47$) (Table 2). In addition, no bacterial colony was detected in the bronchi of vaccinated macaques, whereas a few bacterial colonies were detected in the bronchi of non-vaccinated macaques (Table 1). These findings are compatible with the histological severity.

We analyzed IL-10 production after the infection as it has been reported that IL-10 controlled lung inflammation during influenza virus infection [23, 28]. IL-10 production in nasal swab samples from macaques infected with NL2586 alone was not altered on day 8 after the infection comparing with that before the infection, whereas IL-10 production after the inoculation with NL2586 and *S. pneumoniae* was significantly decreased in macaques with and without vaccination ($P = 0.002$ in NL2586 alone vs. NL2586 + *S. pneumoniae*, $P = 0.02$ in NL2586 alone and Vac-2 + NL2586 + *S. pneumoniae*; Fig. 4). However, vaccinated macaques infected with HPAIV and *S. pneumoniae* showed intermediate IL-10 reduction because of low bacterial growth in the vaccinated macaques (Tables 1 and 2). These findings suggest that *S. pneumoniae* infection suppress IL-10 production in macaques and that low production of IL-10 may enhance inflammation in the lung of unvaccinated macaques as observed in histological results (Fig. 2).

Virus replication in swab samples from cynomolgus macaques after challenge with NL2586 or both NL2586 and Streptococcus pneumoniae

We examined virus replication in nasal swab samples from cynomolgus macaques after challenge with

Table 3 Virus recovery from nasal swabs of macaques inoculated with NL2586

		Virus titer [log 10 ($TCID_{50}$/ml)]									
Inoculation	Animal[1] (dpi)	1	2	3	4	5	6	7	8	10	12
NL2586	327	3.50	3.67	3.00	5.33	3.50	2.67	<	<	<	<
	368	2.67	2.33	2.00	2.23	<	<*	<	<	<	<
	542	<*	<	<*	1.67	1.67	2.50	<	<	<	<
NL2586	406	4.23	2.00	2.50	<*	<	<*	<*	<	<	<
+*S. pneumoniae*	435	3.50	3.00	2.50	2.00	2.50	3.00	<*	<*	<	<
	464	3.33	1.50	2.67	2.50	<*	<*	<	<	<	<
Vac-2	370	2.33	2.33	<	<	<	<	<	<	<	<
NL2586	373	<*	<	<	<	<	<	<	<	<	<
+*S. pneumoniae*	410	<	<	<	<	<	<	<	<	<	<

dpi, days post infection.
The symbol '<' indicates that the virus titer was less than the detection limit (<10 $TCID_{50}$/ml).
The symbol '<*' indicates that one cytopathic effect-positive well was observed in quadruplicate culture of undiluted sample solution.
[1]Each macaque was inoculated with NL2586 (4×10^7 $TCID_{50}$) and/or *S. pneumoniae* (1.2×10^9 CFU) on day 0.

J Med Primatol **39** (2010) 58–70
© 2009 John Wiley & Sons A/S

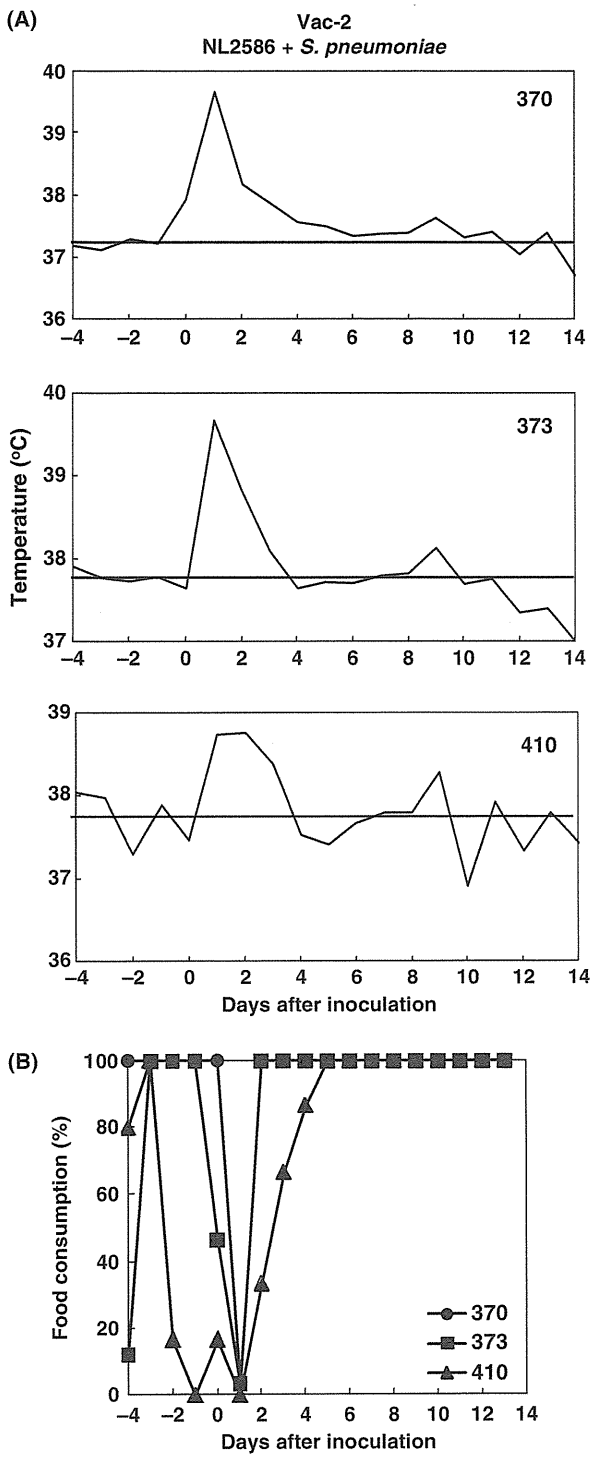

Fig. 5 Body temperatures and food consumption of vaccinated macaques after inoculation of H7N7 HPAIV (NL2586) with *Streptococcus pneumoniae*. Cynomolgus macaques (Nos 370, 373 and 410) were subcutaneously vaccinated twice. Seven weeks after the first vaccination (5 weeks after the second vaccination), NL2586 (4×10^7 $TCID_{50}$) was inoculated onto conjunctivas and into nasal cavities and tracheas with *S. pneumoniae* (1.2×10^9 CFU) into tracheas. (A) Body temperatures were monitored by telemetry transmitters implanted in the peritoneal cavities. Average temperatures of the highest and lowest temperatures on one day are time-dependently shown. Lines drawn horizontally indicate the average temperature levels at pre-infection. (B) Appetite was reflected by the amount of food consumed, which was calculated from the numbers of residual and fed pellets.

NL2586 or both NL2586 and *S. pneumoniae*. The virus was detected in nasal swab samples from the macaques until day 6 after inoculation with NL2586 (average 6 days; Table 3). Similarly, after simultaneous infection with NL2586 and *S. pneumoniae*, the virus was detected in nasal swab samples from the macaques until days 6–8 after the challenge (average 7 days, $P = 0.16$ vs. NL2586 alone). On the other hand, in swab samples from the vaccinated macaques, the virus was detected until day 2 after simultaneous challenge with NL2586 and *S. pneumoniae* (average 1 day, $P = 0.002$ vs. without vaccination). Therefore, it was clearly shown that pre-inoculation with whole particles of Vac-2 decreased H7N7 HPAIV replication in the respiratory tract after simultaneous infection with H7N7 HPAIV and *S. pneumoniae*. In addition, the average weight of vaccinated macaques on day 14 after challenge was 92% of the weight on day 0. Therefore, loss of weight was significantly reduced by vaccination ($P = 0.025$, vs. 88% in unvaccinated macaques as stated above). Furthermore, the average duration of abnormal body temperature after inoculation with NL2586 and *S. pneumoniae* was 2.67 days in vaccinated macaques (Fig. 5A) but 10.67 days in unvaccinated macaques (Fig. 1A) ($P = 0.01$). The average duration of appetite loss was 2.67 days in vaccinated macaques (Fig. 5B) but 7.33 days in unvaccinated macaques (Fig. 1B), although the difference was not statistically significant ($P = 0.06$). Thus, prevention of viral replication by the vaccine would decrease bacterial growth, severity of bacterial pneumonia and morbidity of infection.

Immune responses against HPAIV affected by mixed infection with Streptococcus pneumoniae

We examined immune responses against H7N7 virus and *S. pneumoniae* after infection to see whether mixed infection altered responses against the pathogens. As it was technically difficult to prepare purified antigen of NL2586 for ELISA, we used Vac-2 antigen to examine antibody responses against H7N7 virus. Serum IgG

© 2009 John Wiley & Sons A/S